Dynamics of oligomerization of silicate solution studied by Molecular Dynamics

Frédéric Gruy, Malgorzata Kaminska, Jules Valente

Dynamics of oligomerization of silicate solution studied by Molecular Dynamics

Frédéric Gruy [a](*), Małgorzata Kamińska [a,b], Jules Valente [b]

a - Mines Saint-Etienne, Univ Lyon, CNRS, UMR 5307 LGF, Centre SPIN F - 42023 Saint-Etienne France

b - Solvay, RIC Paris, 52 rue de la Haie Coq, F - 93308 Aubervilliers France

* corresponding author

gruy@emse.fr

0033477420202

ABSTRACT

The main route of silica powder production is the precipitation from sodium silicate solution in the 8-10 pH range. It was earlier established that the oligomerization of the silicate species is an important stage in silica nucleation. We performed molecular dynamics simulations of unsteady silicate solutions at T>1000K to overcome the difficulties encountered in oligomerization experiments (e.g. reliability of the obtained kinetic data). We studied the dynamics of oligomerization for various basic pH, temperature, and silicate concentration values. Based on the Becker-Döring theory of nucleation we now propose a simple reaction mechanism and a quantitative model explaining the evolution of the smaller oligomers concentration with time. The model requires fitting two physical parameters: the kinetic constants of oligomerization and hydrolysis; they depend on the temperature, but not on the size of the oligomer reacting with the monomer. Using the Arrhenius law, we deduce the activation energies for condensation and hydrolysis; we show that the pre-exponential term in the oligomerization rate follows Smoluchowski's theory for Brownian aggregation. Applying the model to the silicate

oligomerization at room temperature, we show that our model agrees with previously published modeling based on energetics considerations. The role of the counter-ions is also confirmed.

Keywords: sodium silicate, oligomerization, molecular dynamics, mechanism, kinetic parameters

Introduction

The control of the precipitation of silica from basic solutions is a challenging task for manufacturers. Nowadays, we dispose of a vast amount of data concerning the growth of silica particles, their aggregation, and agglomeration, as well as the dependence of those steps on experimental conditions [1], [2]. However, we have not yet reached a full understanding of the process. We still need to shed some light on the very first instants of silica precipitation, just after the neutralization of the sodium silicate solution, when the system transformations lead to the formation of silica nanoparticles. Bridging this gap is crucial for full control over the final product morphology.

The well-established theory is that nucleation is an abrupt process, requiring a supersaturation high enough to launch the reaction [3]. Nucleation has been extensively studied for various phase transitions. Numerous theoretical developments are based on the kinetic approach due to Becker and Döring [4]: they consider the nucleation as a polymerization where the elementary step is the reaction between a monomer and a previously formed polymer or oligomer. This approach seems especially suitable for silica nucleation. Therefore the early beginnings of the reaction, consisting of spontaneous, overlapping processes, lead to the generation of a variety of small oligomers [5]. These species, then, transform further via reactions including cyclization (i.e., internal reorganization of species), monomer addition to larger oligomers, and possibly oligomer-oligomer collisions. Monomers contain only one silicon atom, but can be neutral or monocharged depending on the pH (pH<11). Reactions may occur between neutral species or between a neutral and a single-charged species, the second one prevailing at basic pH [6]. If silica nucleation is related to a set of chemical reactions, an appropriate approach is the determination of the rate-limiting, i.e., the slowest step of the whole process. This value is linked to the search of the critical nucleus, which is a very popular notion in nucleation theories.

According to the experimental work of Rothbaum and Rohde [7], the rate-limiting step is the dimerization at pH=7-8 and T<453K, whereas it is the reaction between monomer and dimer for Belton et al. [8] at pH<7 and T<323K. Icopini et al. [9] experimentally show that the rate-limiting step is the reaction between the monomer and the trimer for 3<pH<11 and T=298K.

The discrepancies found in the literature are due to the various techniques used to follow the oligomerization kinetics and the impact of the operational conditions on the precipitation process:

- The experimental studies on the kinetics of the beginnings of silica precipitation mention the induction period, followed by the processes put together into one group classified as "silica condensation". The origin of such simplification lies in the detection limits of experimental methods, which are not able to access the sub-nanometer scale of oligomerization. Consequently, they cannot make a distinction between the early oligomerization reactions. Furthermore, quite possibly, those reactions are not even detected, as they fall in the "induction time" period.
- One of the most critical parameters is the temperature of the reaction mixture. It accelerates the reactions, leading to a much faster system evolution [8], [10]. Nonetheless, some contradictory experimental results question this simple dependency, stressing the role it plays in setting the initial supersaturation [7], [11], [12]. Another crucial factor is the pH of the solution. The majority of studies report on the accelerating effect of implementing a higher pH on silica condensation [11], [13-15] (pH>3). Icopini et al. [9] and Belton et al. [8] have separately shown a linear relationship between the pH and the logarithm of the kinetic constant of the rate-determining step. It is explained as a consequence of the presence of hydroxyl ion, promoting polymerization. Finally, silica concentration, which sets the initial supersaturation, and influences the reaction rate, plays a significant part in the process. Several researchers evoked the positive effect of raising the initial concentration on shortening the induction period (i.e., the time interval before the reaction can be experimentally detected) and accelerating the condensation process [3], [7], [9], [11], [12], [16].

Investigators have tried to estimate the size of the critical nucleus. Iler [3] and Töbler [17] found an experimental value within the range [1.4; 2 nm], i.e 16-50 silicate species per nucleus. However, some researchers questioned these values and found a smaller critical nucleus. Icopini et al. [9] show that the critical nucleus could be the cyclic tetramer, which is more stable than the linear tetramer. Kley et al. [18] agree with Icopini by showing that the induction time for nucleation can be explained by the slow formation of small cyclic oligomers. This is consistent with the reaction mechanism proposed by Belton et al. [8]. It underlines the role of the oligomer cyclization or restructuring in the formation of stable species.

Hence, there is a demand for methods providing access to the molecular details of the processes of interest and especially the formation of the smallest oligomers.

Molecular Dynamics (MD) is a computational method employed to simulate the temporal evolution of the systems at predefined conditions. Solving the equations of motion allows calculating (at each iteration) the positions and velocities of all the atoms in the system. Simultaneously, the reactive potential, with experimental parameters trained for the specific system, account for the interactions between the atoms, including the formation and breakage of bonds. Consequently, we can follow the morphology of clusters evolving from a given initial mixture of molecules. We can, therefore, extract information about the succession of events - the reaction mechanism. If the number of reacting species is large enough, the kinetics of the system simulating a solution can be studied.

The literature provides several examples of MD simulations on the evolution of silicate species. In essence, we can separate such studies into three main groups. The first one implements the Garrofalini-Feuston potential [19], [20]. This interatomic potential is straightforward, and it does not account either for charge transfer or polarizability. It is, however, the subject of a few studies [21], [22], each of which expanded the system size and reached further simulations steps. The most noteworthy is the research published in 2004 by Rao and Gelb [22]. Starting from a set of N_0=729 monomers (only silicic acid), they consider the oligomerization at 1500K<T<2500K, and $0 \leq n_{HS} \leq 26$ for t<15ns (N_0 is the number of silicon atom inside the simulation box, n_{HS} denotes the water-to-silicon ratio, t the time). Rao and Gelb detected in their simulations a cluster of 6.72 nm in length. This species was very elongated and not dense enough to call it a critical cluster or a particle (the possible cause is the primitive reactive potential). However, still, to the best of our knowledge, it is the largest nucleus detected in MD simulations on silicates. This nucleus appeared in the simulation of Rao at a very high temperature of 2500K (to accelerate the reactions) after 12.5ns of simulation time.

The second group of methods implements Car-Parrinello Molecular Dynamics - a technique derived from a combination of Density Functional Theory and MD simulations. This method, much more precise, does not allow reaching advanced simulation times. Trinh et al. [23] and Pavlova et al. [24] focused on the very first instants of the synthesis of zeolites. The former research included small oligomers up to tetramers, while the later limited the study to dimers and trimers. They both concentrated their efforts on determining the reaction mechanism by studying the species privileged within the considered range. They reported the activation energy value for each

oligomer reaction. Pavlova et al. also included the effect of the presence of Na^+ ion, concluding on its repressing impact on dimerization and trimerization. They assigned this finding to the rearrangement of hydrogen bonds of water surrounding reacting species, forced by sodium.

The third family of MD simulations includes the reactive ReaxFF potential, developed by van Duin et al. [25]. We can find two examples of such a study – the one of Jing et al. in 2015 [26] and the more recent study of Du et al. in 2018 [27]. Jing et al. implemented the replica-exchange method to apply the realistic temperatures in their study of the beginning of the zeolite synthesis (T=353-543K; density 10^3 kg/m^3). Their investigation with the water-to-silicon ratio of 5 (300 H_2O, 60 $Si(OH)_4$, 20 NaOH molecules), allowed them to study the evolution of the system, leading to the formation of a cluster built of ~30 Si atoms. A stable state was reached after t>7ns: the mass fraction of oligomers decreased with the mass i, reached a minimum at i=8 (at T=600K), and then increased with i. However, no quantitative information about the kinetics can be obtained from their simulations. They also studied the role of sodium ion and temperature on oligomerization reactions. They noticed that sodium was promoting faster oligomerization: the effect was strong at lower temperatures, and became less significant with the temperature rise.

Then, Du et al. examined the systems with water-to-silicon ratios of 0-9 and temperatures in the range of 1500 to 3000K. Silicate concentration corresponded to systems experiencing gelation (acidic or neutral concentrated solution). Those simplifying and accelerating factors allowed them to study the effect of the applied forcefield. They compared the forcefield of Fogarty et al. [28] and Yeon et al. [29]. Interestingly, even if they did notice that the reaction was launched sooner with the forcefield of Fogarty, the final equilibrium state did not vary in the two cases. They reported the change with time of the various oligomer concentration. Du et al. also examined the impact of temperature, stating the accelerating effect of the rise in temperature on the condensation ratio. Then, they calculated the polymerization rate. They estimated the activation energy of 109kJ/mol for the forcefield of Fogarty and 160kJ/mol for the forcefield of Yeon. Next, examining the technical aspects of their simulation, they observed that in the smaller system (N_0=64 as compared to N_0=512; T=2000K, n_{HS}=3) the polymerization rate is slightly higher, and the number of species fluctuates more. Subsequently, they proved that increasing the amount of water was resulting in a decrease in the final condensation ratio and an increase in the activation energies.

As explained, Molecular Dynamics simulations found in the literature are, in the majority of the cases, limited to the very first instants of the process and the dynamics of acidic or neutral solutions. Therefore, we wish to provide a study collecting the impact of operational conditions

on the dynamics of basic solutions. The current investigation focuses on proposing a simple reaction mechanism, developing a corresponding kinetic model, and estimating the values of kinetic constants.

We focused on the systems with intermediate and high silicate concentrations but without undergoing gelation. In the previous paper [30] we described our MD study on the systems containing sodium silicate and silicic acid and low water content ($0 \leq n_{HS} \leq 2$), i.e. the water concentration C_w<4M. This simplification, i.e applying the lower water content, had been already evoked in the literature (f.ex.,[22], [26], [27]). The selected temperature values were 300K, 600K, 1000K, 1500K, 2000K. Based on the differences in the obtained results we identified two ranges of temperature. Within the [300K-1000K] range, aggregation of sodium silicate molecules occurs whereas silicic acid does not form any oligomers. The small aggregates may undergo restructuring. At the same time, a large aggregate emerges. In the end, an equilibrium between the large and the small aggregates is reached. The process is not sensitive to water content. Within the [1500K-2000K] range, the reaction between monomers and small oligomers with Si-O-Si bonds, i.e. condensation, occurs. Only small oligomers are produced. Water catalyzes the formation of oligomers. The present paper is devoted to the study of the oligomerization of silicate aqueous solution with a high water content, i.e a concentration close to C_w=55M for dilute solutions.

The paper is organized as follows. Section 1 includes a description of materials and methods based on Molecular Dynamics. Section 2 presents some results comprising the effect of the system size, pH, silicate concentration, and temperature on the oligomers morphology and the oligomerization kinetics. In section 3, we discuss those results, proposing a mechanism of oligomerization, corresponding to the operating parameters in the considered range. Section 4 concludes the paper.

1 Materials and methods

In our study, we used the SCM implementation of ReaxFF reactive potential [25], [31], [32] with the forcefield file from Rahnamoun et al. [33] (Si/O/H/Na interactions). Due to the large water content in our system, the number of atoms in the simulation box was very high. Therefore we

performed the majority of simulations on the Occigen supercomputer from GENCI (3.5 Pflop/s, 3576 computing nodes with a total of 85824 cores and 200 To of RAM). The simulations needing less computational resources, e.g. computation of diffusion coefficients, have been performed on the computational cluster (facility) of École des Mines de Saint-Étienne, 'Centaure', composed of 28 computing nodes with a total of 560 cores and 1.8 To of RAM.

First, before each simulation, we packed the molecules into the simulation box with periodic boundary conditions. We set the number of molecules and the size of the box, determining the total concentration of silicate species, C_0. Our systems were composed of $Si(OH)_4$, $Si(OH)_3O^-Na^+$, and H_2O molecules. We set the pH by changing the ratio $R_{b/a}$ of the number of $Si(OH)_3O^-$ ions to $Si(OH)_4$ molecules as follows the equation ($pK_{a,1}$=9.5; T=298K)

$$pH = pK_{a,1} + \log\left(\left[Si(OH)_3O^-\right]/\left[Si(OH)_4\right]\right) \quad (1)$$

As the considered mixtures are aqueous solutions with a density close to 10^3 kg.m^{-3}, we expect the occurrence of the proton transfers. The pH is therefore a meaningful quantity despite the high temperature.

We attempted to repeat each simulation at least two times. Regardless of how many simulations we had (the choice of the repetition number will be explained later), we then calculated the average number of species coming from all the trials. Subsequently, we calculated an average for every forty time steps to smooth the data series and to limit the system fluctuations.

The choice of the simulation parameters

As mentioned before, preparing simulations started by setting the initial number of molecules. We set the pH close to the $pK_{a,1}$, i.e. pH=8.2, 8.7, 9.5, or 9.7. Our simulations included N_0=40, 80, 160, or 400 monomers (N_0 – initial number of monomers).

We set the water content, i.e n_{HS}, considering the simulated mixture as the corresponding silicate solution at room temperature.

To set the concentration, we, then, chose the size, *a*, of the box. We tested the initial concentration, C_0=115 g SiO_2/L (a= 32.7Å for N_0=40), which is an experimentally realistic (but relatively high) concentration, which we then compared with an even lower concentration of 46 g SiO_2/L (a=44.3Å for N_0=40). As expected, increasing the initial concentration resulted in a much more

abrupt system evolution, accelerating the reactions by decreasing distances between the reacting molecules. Thus, in the current investigation, we focus on C_0=115 g SiO_2/L as we did for systems with $0 \le n_{HS} \le 2$ [30].

The position of molecules in the simulation box was randomized.

Having prepared the system, we then chose the technical aspects of simulations. We decided to set the simulation step of 0.25fs (a time step short enough to cover the fastest changes in the reactive system). According to the tests we performed, the simulation step equal to 0.5fs was also suitable for simulations at the lower temperature (T=1000K). The Bond Order cutoff has been set to 0.3 as done by other authors (f.ex.,[26]).

In our investigations, we examined the effect of temperature on silica condensation. Thus, we chose a wide range of values: 1000, 1500, 2000, 2300, 2400, and 2500K. The problem we encountered at the highest temperatures was the destabilization of the reactive system (too high velocities of molecules), which was causing a premature stop of some of our simulations. To avoid this problem, we implemented a pre-equilibration stage before the "actual" simulations. We did not directly set the selected temperature; instead, we gradually increased the temperature from the room temperature T=298K to the temperature of interest within the first 10^4 iteration steps. We applied this technique in the least stable simulations. We compared the evolution of such systems with the systems without the prior pre-equilibration, and we stated that the results coincided. That allowed us to prepare more stable systems, which were less prone to provoke the simulation crash.

Finally, we set the simulation time. It was within the range [1; 20ns] depending on the silicate concentration, the pH, and the temperature.

2 Results

In this section, we present an analysis of the evolution of the system with simulation time. This section only provides the highlights of the system evolution and not a quantitative analysis. To compare the results, we represent them as a normalized quantity, dividing the mass of the clusters or oligomers of a given size by the initial mass of silicate species. If not specified, the solution is initially composed of N_0 monomers.

The effect of N_0

First, we compared the results of simulations for different system sizes (N_0=40 or N_0=160). Figure 1a and b present the results for C_0=115 g SiO2/L, pH=pKa,$_1$, T=2000K, and 1500K. As we can see from the (normalized) evolution of species with simulation time, the size of the simulated system does not seem to play a significant role. What we can notice is slightly higher fluctuations in the case of smaller systems, but the results match well. Oligomers appear and disappear in the course of the oligomerization simulation. The larger the oligomer size is (trimers and tetramers are not shown in the Figure 1a-b for its readibility), the higher are the fluctuations of its number. However, we observe larger oligomers for N_0=160 compared to N_0=40.

Information at the atomic scale

We discuss below the simulations ran at 1000-2000K in more detail as a means of comparison with the previously described systems with n_{HS}<2 [30].

In the course of the simulations, we observed the formation of typical silicate oligomers (with the oxygen Si-O-Si bridges) almost since the beginning of the process. At 1000K, after 0.13ns, an example dimer consisted of an anion and a neutral species, sharing one hydrogen: $(HO)_3$-Si-O-H-O-Si-$(OH)_3$, while after ~0.2ns another dimer already included a typical Si-O-Si bond.

Then, at 1500K, after 0.035ns, we observed dimers formed from two neutral species with a vicinity detected by ReaxFF between two hydrogens: $(HO)_3$-Si-O-H-H-O-Si-$(OH)_3$. After 0.05ns, we observed a trimer with the connections created between sodium ions of neighboring anions. Later, after 0.07ns, we detected a penta-coordinated Si atom, $(HO)_3$Si-O-Si$(OH)_4$, which is an intermediate species in the commonly evoked silicate condensation mechanism (f.ex. Zhang [6]). After 0.14-0.15ns, we already observed a lot of covalent bonds typical for silicate oligomers with a few hydrogen bonds and a few Na^+- Na^+ connections. When we considered the final simulation steps reached, f.ex., after 10ns, we detected only Si-O-Si linkages, forming typical silicate oligomers. As expected, the sodium ions play an important role during the birth and the conformational changes of the oligomer.

For the last temperature under consideration, T=2000K, the obtained results were similar. For example, after 0.25ns of simulation time, we observed a dimer which consisted of two anions, sharing a sodium ion as well as a trimer with one Si-O-Si covalent bond and one penta-coordinated silicon $(HO)_3Si\text{-}O\text{-}Si\text{-}O(H)\text{-}Si(OH)_4$. Then, after ~0.3ns, the ReaxFF detected a dimer and a trimer, both including Si-O-Si covalent bonds only.

To conclude, the species present at the early beginning of the process were forming through either H-H or O-H connections between two neutral or a neutral and an anionic species, or the Na^+-Na^+ connections between two silicates. However, the species with typical oxygen bridge quickly replaced those clusters, and we did not observe the Na^+-Na^+, H-H, and O-H connections in the further stages of the process.

The role of pH in the system evolution

If we vary the initial pH, i.e. the ratio $R_{b/a}$ between the anionic and neutral silicate species concentrations, the oligomer concentration evolution is modified. Three values of pH have been selected: 8.2, 8.7, and 9.7 corresponding to the $R_{b/a}$ values: 0.05, 0.16, and 1.58. Figure 2 presents the normalized monomer concentration versus time for these three pH values and T=2000K. The monomer concentration decreases faster as the pH increases to the $pK_{a,1}$ value. This is consistent with a predominant mechanism based on the efficient collision between the anionic and the neutral silicate species. However, the decrease of the monomer concentration for the pH value equal to 8.2 is significant compared to the other pH values and despite a low $R_{b/a}$ value. As a consequence, the neutral–neutral silicate species collisions could take place, although to a lesser extent, to the oligomer formation at T=2000K. This point will be discussed in section 3.

The role of temperature in the system evolution

We studied the dynamics of the silicate system at T=1000, 1500, 2000, 2200, 2300, 2400, and 2500K. We noticed two different tendencies for a system with C_0=46 g SiO_2/L: in the range 1000-2000K and the range 2000-2500K (figure 3). First, raising the temperature from 1000K to 2000K

results in a higher Si_1 conversion ratio. However, increasing the temperature further, from 2000K to 2500K, does not seem to change the monomer consumption ratio in such a significant way.

At the same time, we have observed that the evolution of larger species ($Si_{n>1}$) varies even between the temperatures in the range 2000-2500K and that the maximum cluster size increases (not shown in this paper).

Interestingly, raising the temperature from 1000K to 1500K seems not to be enough to properly "launch" oligomerization within the simulation duration. We can, though, notice that it is different in the case of a higher concentration (115 g SiO_2/L) presented in Figure 4, where we see a difference for the simulations at those two temperatures. Then, increasing the temperature by the next 500K to T=2000K, we observe a very significant change in the number of consumed monomers, which is in every case higher than for the previously discussed increase from 1000K to 1500K. Subsequently, adding another 500K to reach T=2500K has a smaller, but still a positive impact on the extent of oligomerization. (not shown in Figure 4)

In general, we would expect that applying higher temperatures would increase the velocity of molecules, causing them to collide (and react) with each other more often. Analyzing our results, we could presume that at 1500K as compared to 1000K, the velocities of molecules (and consequently collisions leading to reactions) are slightly higher. Then, at 2000K, this effect is much more significant. However, we enter the temperatures close to the range in which we observe the vibrational excitation of molecules and the resulting destabilization of reacting atoms. That may explain why the differences in the evolution of species are less noticeable for T>2000K. In other words, reactants overcome easily the energy barrier in this range of temperatures.

The effect of water-to-silicon ratio on system evolution

We compared a few simulations corresponding to different H_2O/Si ratios: from silicate systems with low water content, i.e. n_{HS}=0; 0.5; 1; 2, [30] to aqueous silicate system (n_{HS}=29). To investigate the effect of the H_2O/Si ratio, we compared the evolution of species for C_0=115 g SiO_2/L at 1000, 1500, and 2000K. Figure 5 presents the change of the oligomer concentration with time for the three temperatures and three values of n_{HS} (=0, 1, 29). Note that the simulation time range in this figure is shorter than the ones previously shown.

Analyzing these figures briefly, we could draw the first conclusion, stating an evident impact of water, seen more clearly when comparing data from simulations with a low (or no) amount of water (n_{HS}=0; 1) with the realistic conditions (n_{HS}=29).

We can notice that at 1000K, the small amounts of water (n_{HS}=0; 1) provide results similar to each other. The only difference we can see is after the addition of the realistic amount of water (n_{HS}=29), which results in preventing a significant evolution of the system in the investigated time range.

Then, at 1500K, we see that the difference in the extent of oligomerization is already apparent between the n_{HS} in the range 0-1, and it changes again when raising the n_{HS} ratio to 29. In each of those cases, the reaction slows down noticeably to eventually diminish for the simulations with a realistic amount of water.

Finally, at T=2000K, the same tendency (accelerating oligomerization in systems containing less water) is observed, which is, however, less evident than in the previous cases. We can state a difference between simulations with a low (or no) amount of water (n_{HS}=0, 1) and the realistic conditions (n_{HS}=29). They are, nonetheless, closer to each other.

A possible explanation for our observations lies in the reaction mechanism. We should take into consideration that in the oligomerization, water plays not only the role of the carrier in the diffusion processes but also a catalyst in the condensation and a reactant in the hydrolysis reactions. It means that when we add more water to the system, their molecules act as a barrier, preventing reactants from constantly colliding (and consequently reacting) with each other. Moreover, they subsequently privilege hydrolysis of already created covalent bonds (a reaction reverse to oligomerization), impeding the evolution of the system.

To validate this assumption, we looked into the morphology of the system to compare it with previously discussed systems with low water content [30]. We noticed that the aggregates, similar to those observed for low water content systems, were present in the solution only at the early beginnings of simulations. Then, very soon after the start of the calculations, we could already detect the oligomers with typical Si-O-Si bonds. We can, therefore, assign the difference in the evolution of species to the shift in the reaction mechanism in the direction of the classical mechanism of (oligomerization) condensation, which is much slower than aggregation in non-dense medium observed for low water content systems. This effect would be especially evident at 1000K (for low water content systems we detected mostly large aggregates, while at 1500K and

2000K, we already observed some covalent bonds even for low n_{HS} values and very small aggregates.

Computation of the transport properties of silicate species

The diffusion of reactants in the solvent is an important stage in the reaction pathway. It is therefore relevant to compute the diffusivity of the silicate species in water for various temperatures. We computed diffusivities from dedicated simulations.

The diffusion coefficient was estimated using the obtained trajectory file, processed with TRAVIS (an SCM implementation of the command-line tool applied to analyze and visualize trajectories from MD and kMC simulations). The method is based on the Mean Displacement Curve (MDC), relating the displacement of molecules to the diffusion coefficient (derived from Smoluchowski theory) in the following way

$$\left\langle r^2 \right\rangle = 6Dt \tag{2}$$

where $\left\langle r^2 \right\rangle$ denotes mean squared displacement, D - diffusion coefficient, and t - observation time. Table 1 reports the diffusion coefficient for small silicate oligomers at various temperatures.

As expected, the diffusion coefficient values of each species rise with temperature. At room temperature, the differences in the diffusion coefficient for species of studied sizes are small. The diffusion coefficient of silicic acid monomer at 298K is in good agreement with the literature: Cummins [34] (Rebreanu et al. [35]) obtained an experimental value of $D_{Si(OH)4}$(T=298K)=0.8 10^{-9} m^2/s ($1.17 \cdot 10^{-9}$ m^2/s). Then, when we increase the temperature, the differences between oligomers become more noticeable. The diffusion coefficient change, when comparing its values at 298K and 2000K, is around an order of magnitude. This observation is consistent with the MD study of Brodhold and Wood [36], who focused on the self-diffusion of water with a density equal to 10^3 kg/m^3, obtaining the values of D_{H2O}(301 K)= $3.21 \cdot 10^{-9}$ m^2/s and D_{H2O}(1849 K)= $44.2 \cdot 10^{-9}$ m^2/s.

A good approximate for the molecular diffusivity is given by the Stokes-Einstein expression

$$D = k_B T / \left(6\pi\mu R_H\right) \tag{3}$$

Where k_B, μ, and R_H are the Boltzmann constant, the dynamic viscosity of the solvent, and the hydrodynamic radius, respectively. Stokes-Einstein equation is strictly applicable for colloidal suspension, with large sized solute or particle compared to the solvent molecule size. If the ratio of the sizes of the solute and the solvent molecules is smaller than 5, a corrective factor β must be introduced in the Stokes-einstein equation:

$$D = k_B T / \left(6\pi\mu\beta R_H\right) \tag{4}$$

With [37]

$$\beta = \left(3/2R_{H,solv}/R_H + R_H/\left(R_H + R_{H,solv}\right)\right)^{-1} \tag{5}$$

Moreover, the expression (4) is strictly valid only for spherical particles. As a consequence, we apply equation 3 to compute the hydrodynamic radius considered in this paper as an effective hydrodynamic radius.

Considering the dynamic viscosity value of water at 298K, i.e 0.89 mPa.s, we deduce the value of the hydrodynamic radius of the monomer in water: 0.245nm. This value is close to the geometrical radius of the molecule given by Exley et al. (0.231nm) [38] and Siddiqui (0.253nm) [39]. From the monomer diffusion coefficient (at any temperature) and its hydrodynamic radius one can deduce the water dynamic viscosity at the corresponding temperature. Table 2 presents the water viscosity at the applied temperatures, the pressure from Wagner and Pruss [40], and the density.

It is well known that the dynamic viscosity decreases with temperature and increases with pressure. Watanabe et al [41] report the viscosity data versus temperature up to 800K for various pressure values below 100 MPa: the viscosity is almost constant and equal to 0.05 mPa.s beyond the critical temperature of the water. On the other hand, it has been reported that at T=373K the dynamic viscosity is a linear function of the pressure, e.g. the viscosity value at P=1000 MPa is twice the viscosity at P=0.1MPa [42]. These two last behaviors explain the viscosity data reported in Table 2.

From the oligomer diffusion coefficient at T=298K we can deduce the hydrodynamic radius of each selected oligomer from the Stokes-Einstein equation. Table 3 gathers the corresponding data.

We can see that the hydrodynamic radius is not very sensitive to the oligomer size:

$$R_H(i)/R_H(1) \approx i^{0.25} \tag{6}$$

The change of the hydrodynamic radius with i is weaker than the one measured from settling experiments or modeling in colloid science (see, for instance,[43]) or from modeling in polymer physics [44].

To assess the relevance of the Stokes-Einstein equation for our system, we have compared the values of the diffusion coefficient computed from MD (Table 1) with its value calculated from the Stokes-einstein equation using the viscosity data (Table 2) and the hydrodynamic radius data (Table 3). Figure 6 shows the corresponding results. Input data (for T=298K whatever i and for i=1 whatever T) used for the computation of the other diffusion coefficients have been excluded from the figure.

Our data roughly match the Stokes-einstein equation (within 20%). This discrepancy is related to the chosen value of the hydrodynamic radius. This effective value depends on the shape of the molecule and the solvation layer around the molecule: it is expected that the two features depend on the oligomer size, its flexibility, and the temperature.

3 Discussion

We begin the discussion, proposing a modeling methodology for the oligomerization dynamics. Then, we compare the newly formulated model with the model proposed for the systems with much lower water content [30]. Finally, we compare our results with the data provided by other investigators.

A method of quantitative analysis of the small clusters' dynamics ($Si_{N \leq 4}$)

To sum-up the obtained data, we propose a quantitative examination of the kinetics of the small clusters' formation.

First, to limit the number of adjustable values (kinetic constants), aiming at better accuracy and lower computational cost, we reduced the considered reactions to the formation of clusters up to Si_4.

As a reminder, our initial solution contained molecules of $Si(OH)_4$, $Si(OH)_3O^-Na^+$, and H_2O. For clarity reasons, we represent the clusters by the number of silicon atoms they consist of, and we omit other atoms (H, O, Na). The modeling is based on the following features and assumptions, that will be discussed after the application of the model.

i) We considered that the formation of species proceeds via oligomerization (formation of Si-O-Si bonds).

ii) We simplified the reaction scheme: $(i)+(1)\leftrightarrow(i+1)$, with i=1-3 – we considered the formation of species up to Si_4. This reaction scheme leads to a set of ordinary differential equations (ODE) for the oligomer concentrations.

iii) We took into account that, in the presence of the realistic amount of water, the reaction of oligomerization involves (always) an anion and a neutral molecule following Zhang [6].

iv) Considering the high water concentration, proton transfers are very fast compared to the oligomerization rate. Therefore, we account for the acid/base equilibria of the silicate species. The corresponding pKa is a function of i, i.e. the oligomer size. The concentrations of the various oligomers changing with time, the pH is a function of time: it is recalculated at every time step from the pKa definition, the actual concentrations, and the electro-neutrality equations. We also recalculated the concentrations of anions and neutral molecules at each iteration step (they depend on pH). Solute activities when appearing in some equations have been replaced by the concentrations.

v) We assumed that the reaction of hydrolysis involves an anion and water (assumption from Zhang [6]).

vi) We assumed (firstly) that there is no reaction between two neutral species (even if at T=2000K, this could be questionable).

vii) We assumed that the values of the kinetic constants do not depend on i (rule of parsimony). We, therefore, denote them as k_{direct} and $k_{reverse}$. This hypothesis will be discussed later on.

viii) We optimized the kinetic constants' (k_{direct} and $k_{reverse}$) in our ODE solution to match best the MD simulations.

The acid/base equilibria use the values of the pKa for each oligomer and at any temperature. As a reminder the pH is not directly fixed, but the initial base/acid concentrations ratio $R_{b/a}$, i.e

$$\left(A_i^-\right)/\left(A_iH\right) \approx K_{a,i}/\left(H_3O^+\right) \quad (7)$$

for i=1

From Sefcik [45] and Iler's data [3], the pKa,i (before $pKa_{,1}$) at T=298K can be approximated by the expression:

$$pK_{a,i} \approx 7 + 2.5/i^{1/3} \quad (8)$$

At other temperature value, we rewrite the equation (7) as:

$$\left(A_i^-\right)/\left(A_iH\right) = K_{a,i}/\left(H_3O^+\right) = \left[K_{a,1}/\left(H_3O^+\right)\right]\left[K_{a,i}/K_{a,1}\right] \quad (9)$$

And we assume that the $K_{a,i}/K_{a,1}$ ratio does not depend on the temperature; in other words, $K_{a,i}$, and $K_{a,1}$ follow the same change with temperature. H_3O^+ concentration obeys the electroneutrality equation:

$$\sum_{i=1} C_i/\left(\left[K_{a,1}/\left(H_3O^+\right)\right]\left[K_{a,i}/K_{a,1}\right]+1\right) + K_e/\left(H_3O^+\right) = C_{1,0} - \left(Na^+\right) \quad (10)$$

$C_i = \left(A_i^-\right) + \left(A_iH\right)$ is the total concentration of the i-th oligomer, which is the quantity compared with the one given by the MD simulation at each time. From equation 10, we first deduce the $K_{a,1}/\left(H_3O^+\right)$ ratio of the silicate solution and then the concentrations of A_i^- and A_iH at any time.

The oligomer concentrations obey the classical kinetic equations with the initial conditions (oligomer concentrations, but also pH and temperature) depending on the experiment; the temperature is fixed along the process, whereas only the initial pH value is fixed; at a given time, pH is computed from the acid/base equilibria (each oligomer is present as acid and base), mass and charge balance equations. Thus, we have to solve a differential-algebraic system of equations (DAEs). The figures 7, 8 and 9 correspond to the same DAEs, but with various initial conditions.

We used a MATLAB script to estimate the kinetic constants. We set the initial values for each kinetic constant and ran the optimization. To control the accuracy of the fitted values, we calculated the error

$$err = \frac{1}{4}\sum_{i=1}^{4}\sqrt{\frac{1}{M}\sum_{j=1}^{M}\left(C_{i,j}^{model} - C_{i,j}^{MD}\right)^2} \quad (11)$$

for the discretized time, j=[1,M].

We assumed a satisfying fit for err < 0.01 for the systems with (relatively) low fluctuations. At T>1500K, where the results fluctuated more, we accepted higher err (up to 0.03 in the worst cases).

Figures 7a-c show the comparison of the MD-derived system evolution with the data calculated from our simplified model. The abscissa is the simulation time whereas the ordinate is the mass concentration of the i-th oligomer normalized by the total mass concentration at t=0. We only present one simulation for each temperature; this one is selected as the one having the longest duration. We can see that the fit is satisfying. Then, Tables 4a and 4b report on the estimated kinetic constants, including the calculated error.

We shall now comment on these data:

- The noticeable better accuracy for the low temperatures is related to the small reaction advancement, e.g. the normalized monomer concentration remains close to one. The presence of large fluctuations at higher temperatures explains the larger values of the deviation parameter *err*. The kinetic constants belong to a slightly wider range of values: this means that the tabulated values are the mean values +/- 20%.
- Data for N_0=40 and N_0=160 are close to each other according to the reported accuracy.
- As expected, all the kinetic constants increase with the temperature (1000K<T<2000K).
- We observe that the normalized kinetic constant k_{direct} is roughly proportional to C_0 whereas $k_{reverse}$ does not depend on C_0.

The previous simulations were performed with the same initial composition of the solution: only monomers in water. However, we also performed simulations with other initial states. For instance, the model is compared with the MD-simulations for a solution having initially 4 trimers and 870 water molecules ($R_{b/a}$=1; T=2000K) (Figure 8). The kinetic constants are identical to the ones used in figures 7a-c. In this case, the main reaction is the hydrolysis of trimers. We can see that the reaction (condensation or hydrolysis) half-time and the change of oligomer concentration with time are in agreement during the first part of the dynamics; after this period, the model overestimates the hydrolysis of the dimers. It must be underlined that the simulations are performed with a small number of trimer molecules.

Figure 9 presents the normalized monomer concentration versus time for various values of $R_{b/a}$ or pH at T=2000K computed from the model. These data agree with MD simulations data previously reported in section 2.

All these results, i.e. effect of temperature, silicate concentration, pH, and initial composition of the solution on the oligomerization dynamics, show that the proposed model explains well the data issued from the MD-simulations. The model needs only two parameters estimated for each system temperature: k_{direct} and $k_{reverse}$ (Table 4a-b).

The reaction between a monomer and an i-th oligomer consists of the diffusion of two species followed by the formation of the chemical bond. As oligomerization is a part of the nucleation-growth process and as the latter is followed by the agglomeration of the nanoparticles, it would be relevant to use the same formalism for all these collisional, i.e. molecular or particulate, events. Therefore, we choose the Von Smoluchowski formalism [46] for the Brownian coagulation to describe the diffusion and reaction/attachment of entities (molecules or particles). Von Smoluchowski proposed the expression for the kinetic constant or kernel for the collision between two diffusing nanoparticles, denoted i and j:

$$K_{i,j} = K_{i,j}^{0} = 4\pi\left(D_i + D_j\right)\left(R_i + R_j\right) \tag{12}$$

Where D_i and R_i are respectively the diffusion constant and the collisional radius of the nanoparticle i. D_i is given by the Stokes-Einstein equation.

When the nanoparticles are close to each other some forces are acting; certain are attractive as Van der Waals forces, others are repulsive as hydrodynamic or electrical double layer forces; all these forces result in an energy barrier which the nanoparticles must overcome to come in contact. Fuchs [47] and Ottewill and Wilkins [48] have shown that the kinetic constant for Brownian coagulation has to be modified as follows:

$$K_{i,j} = 4\pi\left(D_i + D_j\right)\left(R_i + R_j\right)\exp(-V_{i,j}/kT) \tag{13}$$

where $V_{i,j}$ is the energy barrier height. $V_{i,j}$ is similar to the activation energy for a chemical reaction.

The preexponential term in Eq. 13 can be calculated from the diffusion constants (Table 1) and the collisional/geometrical radii approximated by the expression

$$R_i = R_1 i^{0.4} \tag{14}$$

assuming a spherical-like shape for the flexible oligomers. R_1 value is taken equal to 0.25nm. Figure 10 represents the preexponential term for the monomer/oligomer reaction for various temperatures and the i-th oligomer. We can notice that the preexponential term is very little sensitive to the size of the oligomer. This approach is close to the one of McIntosh [49-50] where the collision event is also separated from the condensation reaction. The author [50] uses the same expression (Eq.12) for the collision dynamics whereas the modeling of the condensation rate requires the generalized transition state theory.

As the reaction/attachment is always the condensation in the monomer-i-th-oligomer pair in our case, the various energy barriers will be replaced by a unique value $E_{a,d}$ (independent of i). The same arguments hold for the hydrolysis of the i-th oligomers.

This discussion justifies point vii.

From the previous discussion, the kinetic constant of an oligomerization step (k_{direct}) obeys the approximate relation:

$$k_{direct} = K_{i,1} = 4\pi\left(D_i + D_1\right)\left(R_i + R_1\right)C_0\alpha\exp(-E_{a,d}/kT) \qquad (15)$$

The k_{direct} values are always several orders of magnitude smaller than the K_0C_0 at the same temperature (Eq.12 and figure 10). This shows that oligomerization is an activated process.

By drawing $k_{direct}/4\pi\left\langle\left(D_i + D_1\right)\left(R_i + R_1\right)\right\rangle_i C_0$ against T^{-1}, the parameters $E_{a,d}$ and α can be estimated: $E_{a,d} = 66 \pm 4$ kJ/mol, and $\alpha = 0.25 \pm 0.05$.

We assume that the kinetic constant of a hydrolysis step ($k_{reverse}$) also obeys the approximate relation:

$$k_{reverse} = A\exp(-E_{a,r}/kT) \qquad (16)$$

An identification procedure of the parameters $E_{a,r}$ and A leads to the inequalities $E_{a,r}$>110 kJ/mol, and A>1500. According to the accuracy of our data, it was not possible to give more definitive values for $E_{a,r}$ and A.

Recently we have studied the dynamics of silicate solution with a smaller water concentration, i.e one-tenth of the liquid water. The temperature set was the same as in the present work. The initial concentration was also equal to C_0=1.9M (115 g SiO_2/L). The main results are the following:

At T<1100K, the kinetic constants of collision in the majority of the cases range from 200 to 400 ns^{-1}, while the kinetic constants of fragmentation range from 50 to 150 ns^{-1}. Kinetic constants do not vary with the water content. Furthermore, the collision kinetic constant decreases slightly as temperature increases, while the fragmentation constant increases slightly as temperature increases. The kinetic constant of the bimolecular collision corresponds to the formation of aggregates: quantitatively, it obeys the Smoluchowski expression including a sticking coefficient α:

$$K_{i,1} = 4\pi\left(D_i + D_1\right)\left(R_i + R_1\right)C_0\alpha \tag{17}$$

α was found equal to 0.2.

At T>1000K, the kinetic constants of collision are noticeably lower (divided by two), while the kinetic constants of fragmentation are of the same order of magnitude as the ones at T<1000K. The covalent bonds appear. The higher the temperature and the higher the water content, the creation of Si-O-Si linkage is faster. The water molecule catalyzes the formation of the Si-O-Si group. This formation, i.e. the condensation reaction, is slow compared to other phenomena with the characteristic time of the order of nanoseconds. Uncertainty for kinetic constant values did not allow us to calculate accurately the activation energy of the condensation reaction in this case. These features observed at low water content are in agreement with the behavior of the silicate system at the larger water concentration studied in this paper.

We now compare our results with the literature, starting with the MD simulations. We focus this analysis on the energy barrier of the oligomerization and hydrolysis of the oligomers. Table 5 gathers some results obtained using different computational methods from the literature.

i) Systems with only silicic acid and water

Rao and Gelb [22] published data obtained for systems with different water content at high temperatures (T=1500, 2000, 2500K). The considered systems contained only silicic acid (acid pH). Therefore, it is difficult to compare their data with our results. In their investigation at T=2500K, C_0=1.8M, and C_w=48M, Rao and Gelb observed a very fast decrease in the monomer concentration followed by a very slow one. This fast reaction occurred within 0.5ns and concerns 25% of the monomer number. This tendency resembles the concentration evolution presented in our investigation (C_0=0.76M, T=2500K, 25%, 0.5ns). Figure 12 in [22] shows the effect of the temperature and the water content on oligomerization. The authors mentioned that

the effect of water content is yet unclear. This point will not be discussed in this paper. At high water content (C_w=48M), the decrease of the monomer concentration seemed to be similar for the three temperatures; a quasi-plateau was reached after 0.2ns. This is very different when compared to our data and confirms that the extent of the reaction between neutral species is limited in basic solution. However, the authors measured that the rate of the monomer concentration initially decreased at the investigated temperatures and then estimated the activation energy of the dimerization of silicic acid (54 kJ/mole). More recently, Du et al. [27] reported on the value 109 kJ/mole also obtained from initial-rate data. This value must be compared with the one estimated by Martin (96 kJ/mole) [21] coming from the kinetic analysis of condensation reactions for systems without water. Zhang [6] proposed the value of 127 kJ/mole. All these data, except the ones from Rao and Gelb, show that the neutral mechanism, i.e. the reaction between neutral species, is not favored when compared to the anionic mechanism (Table 5).

ii) silicic acid/silicate anion/water systems

The data from Trinh [23], Zhang [6], Pavlova [24], and Moqadam [51] show that the energy barrier is not sensitive to the size i of the small oligomer participating in the reaction $(i)+(1)\rightarrow(i+1)$; our value (66kJ/mole) is within the range proposed by these authors [53;81 kJ/mole]. More recently, McIntosh [49] has performed an ab initio study that considers all the possible oligomerization reactions including cyclisations; solvent effects were accurately taken into account. Energy barriers for the formation of linear oligomers have been estimated within the range [37; 74 kJ/mole]. It must be emphasized that the author made a distinction between the reaction $(1)^-+(i)\rightarrow(i+1)^-$ and the reaction $(1)+(i)^-\rightarrow(i+1)^-$.

Data concerning oligomer's hydrolysis are less common in the literature. Zhang [6] and Trinh [23] reported the following values for the energy barrier for dimer, trimer, and tetramer: 77, 69, 87 kJ/mole respectively. These activation energies are at least 16kJ/mole higher than the ones for oligomerization. The deviation between the energy barriers of condensation and hydrolysis explains the low rate of hydrolysis for common temperature values used in oligomerization experiments.

Now, to compare our results with experimental data, we encounter some limitations. Based on the experimental results, several researchers proposed simple kinetic laws and models attempting to describe the kinetics of the monomers' disappearance in the course of silica precipitation. This experimental data, in most cases, came from the silico-molybdate method. However, sometimes, it was combined with additional, complementary analyses. The critical point is the apparent weakness of the molybdic acid method, resulting from the definition of so-called "monomeric" species. In practice, this method detects not only the monomer but also the dimer and possibly larger species up to tetramers. In most studies, the authors did not make any distinction between small oligomers, calling them "molybdate-reactive" or "monomeric" silicic acid. Most often the investigators focus their study on the nucleation, i.e. on the formation of supposed large oligomers.

The researchers derived the majority of the reported models, based on the method introduced by Goto [13], summed-up in the general equation

$$-dC_1 / dt = k\left(C_1 - C_s\right)^n \tag{18}$$

where C_S is silica solubility, C_1 is the concentration of molecularly dispersed silica (monomer), k – kinetic constant, and n denotes reaction order. If $C_1 >> Cs$,

$$-dC_1 / dt = k\,C_1^n \tag{19}$$

After integration,

$$\left(n-1\right)kC_0^{n-1}t = \left(C_0 / C_1\right)^{n-1} - 1 \tag{20}$$

Different values have been proposed for the order of reaction for oligomerization with pH>7. For instance, Goto [13], Okamoto et al. [14], Kitahara[10] have proposed the value 3, whereas Rothbaum and Rohde [7] proposed the value 2 for the slow dimer formation and $n \geq 2$ for the fast formation of larger oligomers. Icopini et al. [9] have proposed the value 4: this may be explained as the slow formation of cyclic tetramer where the monomer, dimer, and trimer are almost at equilibrium; the cyclic tetramer would be considered as the critical nucleus for the silica nucleation. The most commonly evoked study for the experimentally-derived values for the condensation energy barrier of Iler [3] reports on a value of 63 kJ/mol, very close to our result. Despite all the efforts of investigators, no quantitative data about the first instants of oligomerization in basic silicate solutions are available.

Considering that the activation energies computed from our data are consistent with those provided by Trinh and Zhang determined at T=350K, we have calculated the concentration profiles for the smallest oligomers at T=298K. These will be compared with the ones issued from McIntosh's work.

Figure 11 represents the normalized mass concentration versus time for mono, di-, tri-, and tetramers. The solid line corresponds to pH=$pK_{a,1}$=9.5 at t=0, and a closed system (as MD simulations); the dashed line corresponds to pH=9.5 kept constant during the process. It should be underlined that the rate of hydrolysis for T=298K is negligible when considering the oligomerization rate ($k_{reverse}$=0 does not change plots in figure 11). Keeping identical the pKa values for the various oligomers does not change noticeably plots in figure 11.

All the figures show that after a short period corresponding to the formation of all oligomers, their concentrations vary slightly. It seems that the system shows two time scales. This is due to the consumption of the monomers, slowing down the oligomerization. If the system is closed, the pH changes with time, and the monomer concentration reaches a quasi-plateau; this is not the case if the pH of the system is kept constant along the process. In fact, in a closed system, the pH is increasing with time, all the silicate species become negatively charged making difficult the consumption of monomers; in an open system (pH=$pK_{a,1}$ or $R_{b/a}$=1), there is always neutral and charged monomers in the same ratio.

Figure 12 presents the concentration change with time at pH=8.5 or $R_{b/a}$=0.1 and C_0=1M. A log-log plot and the number concentration as the ordinate have been chosen for comparison with the results of McIntosh (figure 4 in [50]). At pH=8.5 or $R_{b/a}$=0.1, one obtains an asymptotic behavior for the oligomer concentrations which is close to the one observed at pH=9.5; only the (first) time scale is 2-3 higher than for pH=9.5.

It can be noted that our simple model reproduces McIntosh's data. As a reminder, our model does not differentiate the various configurations of a given i-th oligomer. The relative location of the curves for the different concentrations are the same in the two investigations. However, the main difference lays in the time scale: oligomerization is 500 times faster in the work of McIntosh. As the time scale in our model is directly related to k_{direct} (k_{direct}>>$k_{reverse}$ at T=298K), k_{direct} is 500 times larger following the research of McIntosh. We may point to two possible reasons: the theoretical equation for k_{direct} and the data set needed in this expression.

i) The equation for k_{direct}: McIntosh considers the oligomerization as a two successive steps process: association/dissociation of a weakly linked oligomer pair and

condensation inside the oligomer pair. The latter is a unimolecular reaction described through the generalized transition state theory (G-TST). The final expression for k_{direct} is closed to the expression (15) but differs in the presence of the transmission coefficient and the ratio of partition functions of the pair at the actual and initial states in G-TST. The ratio of the partition functions is close to one whereas the transmission coefficient value may attain 10^3 at room temperature. The transmission coefficient decreases as the temperature increases and is close to one if T>1000K.

ii) Data set: the activation energy value in (15) leading to the same time scale as McIntosh is equal to 48 kJ/mole. It corresponds roughly to the average value of the energy barrier of each (i)+(1)→ (i+1) reaction. This means that the difference between the activation energies would be the main reason for the different time scales observed in our work and the investigation of McIntosh. It seems that the work of McIntosh does not consider the specific contribution of counter-ions, i.e. cations, to the activation energy for condensation. Zhang [6] and Pavlova [24] have shown that the presence of Li^+ and Na^+ cations leads to an increase of the activation energy value by about 40 kJ/mole for Li^+ and 20 kJ/mole for Na^+. Mai et al. [53] and Ciantar et al. [54] have carefully analysed the role of organic template cations on the oligomerization dynamics. Each oligomerization reaction consists of two elementary steps: the formation of a five-coordinated intermediate followed by the removal of water. Sodium ion and organic templates have a differentiated impact on the first step whereas the activation barrier of the second step seems not to be affected by the cations. Thus, when considering the formation of large oligomers, the content of the oligomer solution appears highly dependent on the cation.

4 Conclusions

From MD simulations performed at high temperatures and an analysis of the kinetic data, we proposed a simple reaction mechanism and the corresponding ODE set containing only two kinetic parameters depending on the temperature. We have shown that the kinetic constant of the monomer-i-th-oligomer reaction may be expressed using the Arrhenius law. An activation energy value is deduced; we have established that the pre-exponential term is compatible with the model of Brownian aggregation from Smoluchowki. The application of the model to oligomerization at

room temperature results in data in agreement with the research of Trinh et al. [23], Zhang [6], Pavlova et al. [24], and McIntosh [50]. In particular, the last ones are based on a detailed analysis of the mechanism of oligomerization and the determination of the corresponding activation energies by using quantum mechanics methods. The activation energy value issued from our work may be considered as their average value.

The kinetic analysis has been restricted to the formation of the smallest oligomers ($i<5$). Tetramers are often considered as an important intermediate species, perhaps the critical nucleus, in the nucleation study. Due to the limitations of our MD simulations (small-sized systems, short simulation time) formation of larger oligomers is less frequent; therefore a classical kinetic analysis cannot take them into account. On the other hand, a statistical analysis of their formation and the analysis of their morphology change is possible. They will make possible the profound comparison with the mechanisms proposed by the cited authors and based only on energetics considerations.

Acknowledgments

The authors thank Solvay Company and the Agence Nationale Recherche et Technologie (CIFRE 2016-0186) for their financial support of this project. They also thank CINES agency and the computational resources GENCI (project A0050910520) for access to Occigen computer.

5 References

[1] J. Schlomach and M. Kind, "Investigations on the semi-batch precipitation of silica.," J. Colloid Interface Sci., vol. 277, no. 2, pp. 316–326, 2004

[2] J. Valente, F. Gruy, P. Nortier, and E. Allain, "Evidence of structural reorganization during aggregation of silica nanoparticles," Colloids and Surf. A: Physicochem. Eng. Asp., vol. 468, pp. 49–55, 2015.

[3] R. K. Iler, The Chemistry of Silica: Solubility, Polymerization, Colloid and Surface Properties and Biochemistry of Silica. New York: Wiley-Interscience, 1979.

[4] R. Becker and W. Döring, "Kinetische Behandlung der Keimbildung in übersättigten Dämpfen," Ann. Phys., vol. 416, no. 8, pp. 719–752, 1935.

[5] D. J. Belton, O. Deschaume, and C. C. Perry, "An overview of the fundamentals of the chemistry of silica with relevance to biosilicification and technological advances," FEBS J., vol. 279, no. 10, pp. 1710–1720, 2012.

[6] X. Zhang, "Kinetic Monte Carlo Modelling of The Initial Stages of Zeolite Synthesis,", PhD thesis, Eindhoven University of Technology, Eindhoven, 2012.

[7] H. P. Rothbaum and A. G. Rohde, "Kinetics of silica polymerization and deposition from dilute solutions between 5 and 180°C," J. Colloid Interface Sci., vol. 71, no. 3, pp. 533–559, 1979.

[8] D. J. Belton, O. Deschaume, S. V. Patwardhan, and C. C. Perry, "A solution study of silica condensation and speciation with relevance to in vitro investigations of biosilicification., A Solution Study of Silica Condensation and Speciation with relevance to in vitro investigations of biosilicification," J. Phys. Chem. B, 114, no. 31, pp. 9947–9955, 2010.

[9] G. A. Icopini, S. L. Brantley, and P. J. Heaney, "Kinetics of silica oligomerization and nanocolloid formation as a function of pH and ionic strength at 25°C," Geochim. Cosmochim. Acta, vol. 69, no. 2, pp. 293–303, 2005.

[10] S. Kitahara, "The polymerization of silicic acid obtained by the hydrothermal treatment of quartz and the solubility of amorphous silica," Rev Phys Chem Jpn., vol. 30, pp. 131–137, 1960.

[11] A. Makrides, M. Turner, and J. Slaughter, "Condensation of Silica from Supersaturated Silicic-Acid Solutions," J. Colloid Interface Sci., vol. 73, no. 2, pp. 345–367, 1980.

[12] H. P. Rothbaum and R. D. Wilson, "Effect of temperature and concentration on the rate of polymerisation of silica in geothermal waters," Geochemistry, vol. 218, pp. 37–43, 1977.

[13] K. Goto, "Effect of pH on Polymerization of Silicic Acid," J. Phys. Chem., vol. 60, no. 7, pp. 1007–1008, 1956.

[14] G. Okamoto, T. Okura, and K. Goto, "Properties of silica in water," Geochim. Cosmochim. Acta, vol. 12, no. 1–2, pp. 123–132, 1957.

[15] H. Baumann, "Polymerisation und Depolymerisation der Kieselsäure unter verschiedenen Bedingungen," Colloid Polym. Sci., vol. 162, pp. 28–35, 1959.

[16] A. D. Bishop and J. L. Bear, "The thermodynamics and kinetics of the polymerization of silicic acid in dilute aqueous solution," Thermochim. Acta, vol. 3, no. 5, pp. 399–409, 1972.

[17] D. J. Tobler, S. Shaw, and L. G. Benning, "Quantification of initial steps of nucleation and growth of silica nanoparticles: An in-situ SAXS and DLS study," Geochim. Cosmochim. Acta, vol. 73, no. 18, pp. 5377–5393, 2009.

[18] M. Kley, A. Kempter, V. Boyko, and K. Huber, "Mechanistic Studies of Silica Polymerization from Supersaturated Aqueous Solutions by Means of Time-Resolved Light Scattering," Langmuir, vol. 30, no. 42, pp. 12664–12674, 2014.

[19] S. H. Garofalini and H. Melman, "Applications of Molecular Dynamics Simulations to Sol-Gel Processing," MRS Online Proc. Libr. Arch., vol. 73, Jan. 1986, doi: 10.1557/PROC-73-497.

[20] B. P. Feuston and S. H. Garofalini, "Onset of polymerization in silica sols," Chem. Phys. Lett., vol. 170, no. 2–3, pp. 264–270, 1990.

[21] G. E. Martin and S. H. Garofalini, "Sol-gel polymerization: analysis of molecular mechanisms and the effect of hydrogen," J. Non-Cryst. Solids, vol. 171, no. 1, pp. 68–79, 1994.

[22] N. Z. Rao and L. D. Gelb, "Molecular Dynamics Simulations of the Polymerization of Aqueous Silicic Acid and Analysis of the Effects of Concentration on Silica Polymorph Distributions, Growth Mechanisms, and Reaction Kinetics," J. Phys. Chem. B, vol. 108, no. 33, pp. 12418–12428, 2004.

[23] T. T. Trinh, A. P. J. Jansen, R. A. van Santen, and E. J. Meijer, "The role of water in silicate oligomerization reaction," Phys. Chem. Chem. Phys., vol. 11, no. 25, pp. 5092–5099, 2009.

[24] A. Pavlova, T. T. Trinh, R. A. van Santen, and E. J. Meijer, "Clarifying the role of sodium in the silica oligomerization reaction," Phys. Chem. Chem. Phys., vol. 15, no. 4, pp. 1123–1129, 2013.

[25] A. C. T. van Duin, S. Dasgupta, F. Lorant, and W. A. Goddard, "ReaxFF: A Reactive Force Field for Hydrocarbons," J. Phys. Chem. A, vol. 105, no. 41, pp. 9396–9409, 2001.

[26] Z. Jing, L. Xin, and H. Sun, "Replica exchange reactive molecular dynamics simulations of initial reactions in zeolite synthesis," Phys. Chem. Chem. Phys., vol. 17, no. 38, pp. 25421–25428, 2015.

[27] T. Du, H. Li, G. Sant, and M. Bauchy, "New insights into the sol-gel condensation of silica by reactive molecular dynamics simulations," J. Chem. Phys., vol. 148, no. 23, p. 234504, 2018.

[28] J. C. Fogarty, H. M. Aktulga, A. Y. Grama, A. C. T. van Duin, and S. A. Pandit, "A reactive molecular dynamics simulation of the silica-water interface," J. Chem. Phys., vol. 132, no. 17, p. 174704, 2010.

[29] J. Yeon and A. C. T. van Duin, "ReaxFF Molecular Dynamics Simulations of Hydroxylation Kinetics for Amorphous and Nano-Silica Structure, and Its Relations with Atomic Strain Energy," J. Phys. Chem. C, vol. 120, no. 1, pp. 305–317, 2016.

[30] M. Kaminska, F. Gruy and J. Valente, "Dynamics of non-dense sodium silicate - water system studied by molecular dynamics," Colloids and Surfaces A: physicochemical and engineering aspects, vol.603, pp. 125226, 2020

[31] K. Chenoweth, A. C. T. van Duin, and W. A. Goddard, "ReaxFF Reactive Force Field for Molecular Dynamics Simulations of Hydrocarbon Oxidation," J. Phys. Chem. A, vol. 112, no. 5, pp. 1040–1053, 2008.

[32] ReaxFF. SCM, Theoretical Chemistry, Vrije Universiteit, Amsterdam, The Netherlands, http://www.scm.com.

[33] A. Rahnamoun and A. C. T. van Duin, "Reactive Molecular Dynamics Simulation on the Disintegration of Kapton, POSS Polyimide, Amorphous Silica, and Teflon during Atomic Oxygen Impact Using the Reaxff Reactive Force-Field Method," J. Phys. Chem. A, vol. 118, no. 15, pp. 2780–2787, 2014.

[34] K. M. Cummins, "Silicic and germanic acids : laboratory determination of their molecular diffusivities and field study of their benthic fluxes along the California margin," M.S. thesis, University of Southern California, 2019

[35] L. Rebreanu, J.-P. Vanderborght, and L. Chou, "The diffusion coefficient of dissolved silica revisited," Mar. Chem., vol. 112, pp. 230–233, 2008

[36] J. Brodholt and B. Wood, "Molecular dynamics of water at high temperatures and pressures," Geochim. Cosmochim. Acta, vol. 54, no. 9, pp. 2611–2616, 1990

[37] Timothy D.W. Claridge, in High-Resolution NMR Techniques in Organic Chemistry (Third Edition), Elsevier Science, 2016

[38] C. Exley, G. Guerriero, X. Lopez, "Silicic acid: The omniscient molecule," Science of the Total Environment, vol.665, pp. 432–437, 2019.

[39] K. S. Siddiqui, "What are dimensions of ortho-silicic acid?," ResearchGate. https://www.researchgate.net/post/What_are_dimensions_of_ortho-silicic_acid (accessed Sep. 14, 2020)

[40] W. Wagner and A. Pruss, The IAPWS Formulation 1995 for the Thermodynamic Properties of Ordinary Water Substance for General and Scientific Use, J. Phys. Chem. Ref. Data, Vol. 31, No. 2, pp. 387-535, 2002.

[41] K. Watanabe, Y. Niibori and T. Hashida, "Numerical Study on Heat Extraction from Supercritical Geothermal Reservoir," Proceedings World Geothermal Congress 2000 Kyushu - Tohoku, Japan, 2000.

[42] https://www.engineeringtoolbox.com/waterdynamic-kinematic-viscosity-d_596.html

[43] F. Gruy and P. Cugniet, "Experimental study of small aggregate settling," J. Colloid and Interf. Sci., vol.272, pp. 465-471, 2004.

[44] M. Nygaard, B.B. Kragelund, E. Papaleo and K. Lindorff-Larsen, "An Efficient Method for Estimating the Hydrodynamic Radius of Disordered Protein Conformations," Biophysical Journal vol.113, pp. 550–557, 2017.

[45] J. Sefcik and A. V. McCormick, "Thermochemistry of aqueous silicate solution precursors to ceramics," AIChE J, vol. 43, no. 11, pp. 2773–2784, 1997.

[46] M. V. Smoluchowski, "Drei Vortrage uber Diffusion, Brownsche Bewegung und Koagulation von Kolloidteilchen," Z. Phys., vol. 17, pp. 557–585, 1916.

[47] N. Fuchs, "Über die Stabilität und Aufladung der Aerosole," Z. für Phys., vol. 89, pp. 736–743, 1934.

[48] R. H. Ottewill and D. J. Wilkins, "Studies on a flow method for particle counting in colloidal systems," J. Colloid Sci., vol. 15, no. 6, pp. 512–524, 1960.

[49] G.J. McIntosh, "Theoretical investigations into the nucleation of silica growth in basic solution; part I – ab initio studies of the formation of trimers and tetramers," Phys. Chem. Chem. Phys, vol.15, pp. 3155-3172, 2013.

[50] G.J. McIntosh, "Theoretical investigations into the nucleation of silica growth in basic solution; part II –derivation and benchmarking of a first principles kinetic model of solution chemistry," Phys. Chem. Chem. Phys, vol.15, pp. 17496-17509, 2013.

[51] M. Moqadam, E. Riccardi, T. T. Trinh, P.-O. Åstrand, and T. S. van Erp, "A test on reactive force fields for the study of silica dimerization reactions," J. Chem. Phys., vol. 143, no. 18, p. 184113, 2015.

[52] T. T. Trinh, A. P. J. Jansen, and R. A. van Santen, "Mechanism of Oligomerization Reactions of Silica," J. Phys. Chem. B, vol. 110, no. 46, pp. 23099–23106, 2006.

[53] N.L. Mai, H.T. Do, N.H. Hoang, A.H. Nguyen, K-Q Tran, E.J. Meijer, T. T. Trinh, "Elucidating the role of Tetraethylammonium in the silicate condensation reaction from Ab Initio molecular dynamics simulations" J. Phys. Chem. B, vol. 124, pp. 10210–10218, 2020.

[54] a. M. Ciantar, T.T. Trinh, C. Michel, P. Sautet, C. Mellot-Draznieks, C. Nieto-Draghi, « Impact of organic templates on the selective formation of zeolithe oligomers », Angew. Chem., 133, pp7187-7192, 2021.

b. M. Ciantar, C. Mellot-Draznieks, C. Nieto-Draghi, "A Kinetic Monte Carlo Simulation Study of Synthesis Variables and Diffusion Coefficients in Early Stages of Silicate Oligomerization", J. Phys. Chem. C, vol. 119, no. 52, pp. 28871–28884, 2015.

List of Tables

List of Figures

N_0=40 green: monomer blue: dimer

a. C_0=115g/L, pH=pK_{a1}, T=2000K
b. C_0=115g/L, pH=pK_{a1}, T=1500K

Figure 2: Normalized mass concentration of monomer versus simulation time for three values of pH: 8.2 (black), 8.7 (red) and 9.7 (blue). C_0=115g/L, T=2000K

Figure 3: Normalized mass concentration of monomer versus simulation time for five values of temperature: 1000K (black), 1500K (red) , 2000K (green), 2300K (blue), 2500K (magenta). C_0=46g/L, pH=pK_{a1}.

Figure 4: Normalized mass concentration of monomer versus simulation time for three values of temperature: 1000K (black), 1500K (red) , 2000K (green). C_0=115g/L, pH=pK_{a1}.

Figure 5: Normalized mass concentration of monomer versus simulation time for three values of water content and three values of temperature. C_0=115g/L, $R_{b/a}$=1.

T= 1000K (black), 1500K (red), 2000K (green)

n_{HS}=0 (dashed line, N_0=64), 1 (solid line, N_0=64), 29 (bold and solid line, N_0=160); Note that the system size doesn't change the results.

Figure 6: diffusion coefficient computed following Stokes-Einstein equation versus the one from MD simulations. Unit: m^2/s

Figure 7a: normalized mass concentration of oligomer versus time (N_0=160, C_0=115g/L, $R_{b/a}$=1) for T=2000K.

black: monomer; red: dimer; green: trimer; blue: tetramer;

solid line: model; fluctuating line: MD-simulation

Figure 7b: normalized mass concentration of oligomer versus time (N_0=40, C_0=115g/L, $R_{b/a}$=1) for T=1500K.

black: monomer; red: dimer; green: trimer; blue: tetramer;

solid line: model; fluctuating line: MD-simulation

Figure 7c: normalized mass concentration of oligomer versus time (N_0=40, C_0=115g/L, $R_{b/a}$=1) for T=1000K.

black: monomer; red: dimer; green: trimer; blue: tetramer;

solid line: model; fluctuating line: MD-simulation

Figure 8: initial state: 4 trimer and 870 H_2O molecules

normalized mass concentration of oligomer versus time (C_0=46g/L; $R_{b/a}$=1) for T=2000K.

black: monomer; red: dimer; green: trimer; blue: tetramer;

solid line: model; dotted line: MD-simulation

Figure 9: monomer concentration versus time for various values of $R_{b/a}$ or pH. T=2000K, C_0=115g/L.

MD simulation versus modelling (solid line)

(R, pH) values: (0.05, 8.2) (black), (0.16, 8.7) (red) and (1.58, 9.7) (green)

Figure 10: the pre-exponential term of the kinetic constant (normalized by $1/C_0$) of the monomer/oligomer reaction versus the temperature for several small oligomers:

i=1 (black dot) i=2 (red dot) i=5 (green dot) i=10 (blue dot)

Figure 11: normalized mass concentration versus time C_0=2M, T=298K, max(i)=10

Solid line: $pH_{initial}=pK_{a1}=9.5$, closed system

Dashed line: $pH_{initial}=pK_{a1}=9.5$, open system (pH = 9.5 along the process)

i=1: black i=2: red i=3: green i=4: blue

Figure 12: normalized number concentrations versus time

pH=8.5 C_0=1M T=298K, max(i)=4 ([50], figure 4)

i=1: black i=2: red i=3: green i=4: blue

Table 1: The values of the diffusion coefficient [10^{-9} m^2/s] estimated for silica oligomers at different temperatures.

Oligomer / T(K)	298	1000	1500	2000
Monomer	1.0	16.6	23.6	28.5
Charged monomer	0.836	15.6	22.8	29.3
Dimer	0.838	12.4	18.6	26.9
Linear pentamer	0.696	9.16	12.3	26.1
Branched pentamer	0.67	8.81	12.4	23
Cyclic pentamer	0.638	8.58	11.9	25
Linear decamer	0.62	7.25	10.1	20.2

Table 2: Dynamic viscosity of water for various temperatures and pressures at constant density.

T (K)	298	1000	1500	2000
P (MPa)	0.1	1412	2295	3060
ρ (Kg/m^3)	1000	1000	1000	1000
μ (mPa.s)	0.89	0.18	0.19	0.21

Table 3: Hydrodynamic radius of i-oligomers computed from diffusivity data at T=298K

i	1	1 (ion)	2	5 (linear)	5 (branched)	5 (cyclic)	10 (linear)
R_H(nm)	0.245	0.295	0.295	0.352	0.366	0.384	0.395

Table 4a-b: List of the estimated kinetic constant values for the $Si(OH)_4/Si(OH)_3ONa/H_2O$ systems

N_0	T(K)	$k_{direct}(ns^{-1})$	$k_{reverse}(ns^{-1})$	err
40	1000	0.03	0.003	0.015
160	1000	0.02	0.003	0.008
40	1500	0.3	0.08	0.026
160	1500	0.25	0.05	0.007
40	2000	2.5	3	0.028
160	2000	2.5	2	0.023

Table 4a: k_{direct} is the kinetic constant normalized with (the inverse of) the total initial concentration (for the bimolecular collision). This initial concentration is equal to C_0=1.9M (115gSiO_2/L).

N_0	T(K)	$k_{direct}(ns^{-1})$	$k_{reverse}(ns^{-1})$	err
40	1000	0.01	0.003	0.0064
40	1500	0.045	0.03	0.013
40	2000	1.5	4	0.019
40	2300	0.6	1.2	0.029
40	2500	1.5	3	0.033

Table 4b: The initial concentration is equal to C_0=0.76M (46gSiO_2/L).

Table 5: Examples of activation energy values for the formation of linear oligomers reported in the literature.

Reference	**Method**	**E_a values [kJ/mole]**
1994, Garofalini and Martin [21]	MD, FG forcefield Silicic acid, sol-gel	96 without water
2004, Rao and Gelb [22]	MD, FG forcefield Silicic acid	54 (n_{HS}=26) with water
2018, Du et al. [27]	MD, ReaxFF Silicic acid, sol-gel	109(forcefield of Fogarty [28]) 160 (forcefield of Yeon [29])
2015, Moqadam et al. [51]	DFT	65 (1+1) anionic mechanism, Na^+
2013, Pavlova et al. [24]	Ab initio MD, explicit water	81 (1+1) 75 (1+2) anionic mechanism, Na^+
2009, Trinh et al. [23] without Na^+ 2012, Zhang [6] See also: 2020, Mai et al. [53] with organic template (cation)	CPMD, explicit water	61 (1+1) 53 (1+2) 56 (1+3) anionic mechanism without Na^+ 127 (1+1) 128 (1+2) neutral mechanism
2006, Trinh et al. [52]	DFT	56-99 (COSMO model, anionic mechanism)
2013, McIntosh [49]	Ab initio, QM	42 ($1+2^-$) 63 (1^-+2) 74 ($1+3^-$) 37 (1^-+3) 62 ($1+3^-$) branched tetra 31 (1^-+3) branched tetra Without Na^+

Reference	**Method**	**E_a values [kJ/mole]**
2021, Ciantar [54] without and with organic templates (cations)	DFT, kMC	65 (1+1) 75 (1+2) 73 (1+3) anionic mechanism without cation Data extracted from a set of 258 reactions with 239 n-oligomers (n<9)

Notation: (i+j): reaction between i-oligomer and j-oligomer.

Figure 1: Normalized mass concentration versus simulation time for two values of N_0.

N_0=160 black: monomer red: dimer

N_0=40 green: monomer blue: dimer

c. C_0=115g/L, pH=pK_{a1}, T=2000K

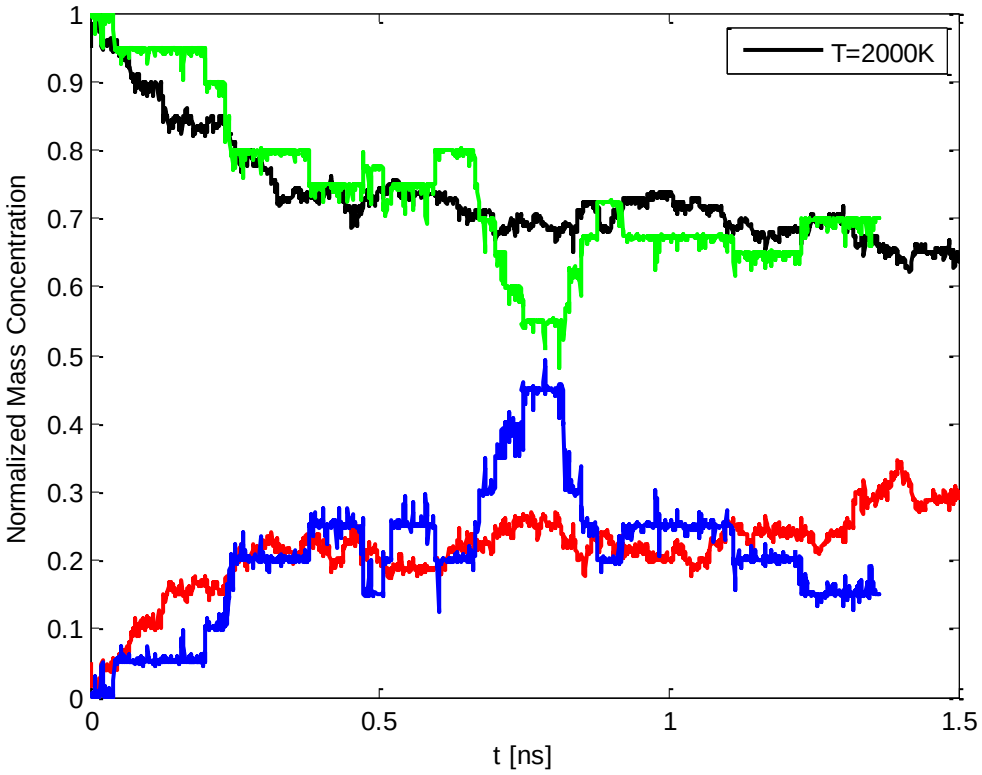

d. C_0=115g/L, pH=pK_{a1}, T=1500K

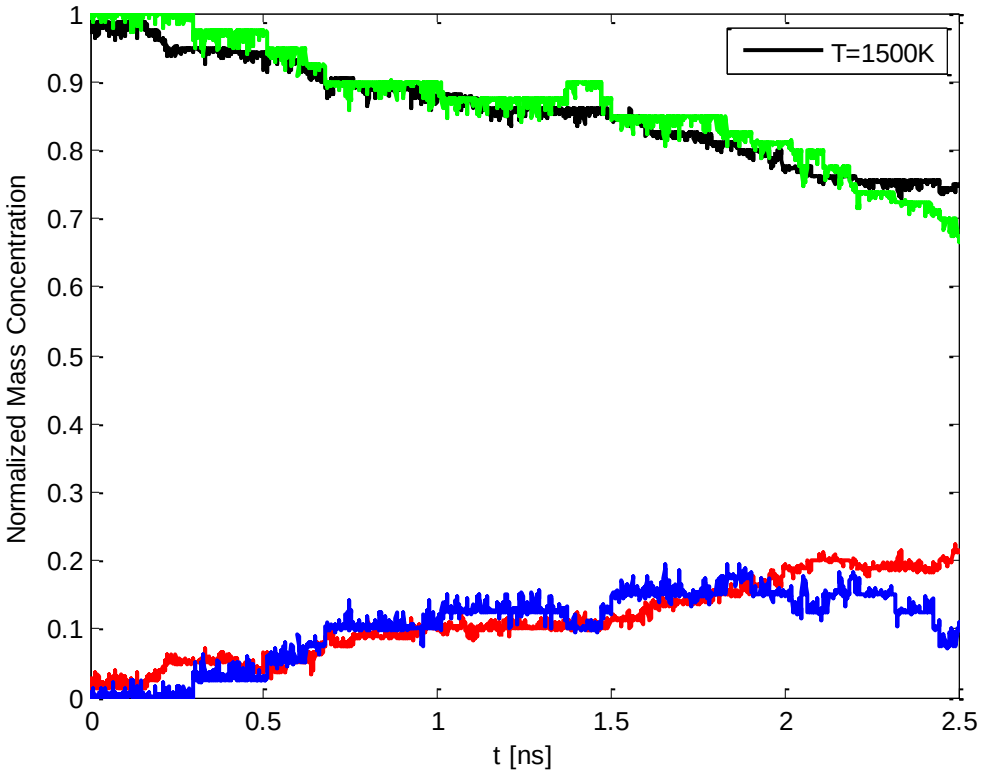
T=1500K
Normalized Mass Concentration
t [ns]
0
0.1
0.2
0.3
0.4
0.5
0.6
0.7
0.8
0.9
1
0
0.5
1
1.5
2
2.5

Figure 2: Normalized mass concentration of monomer versus simulation time for three values of pH: 8.2 (black), 8.7 (red) and 9.7 (blue). C_0=115g/L, T=2000K

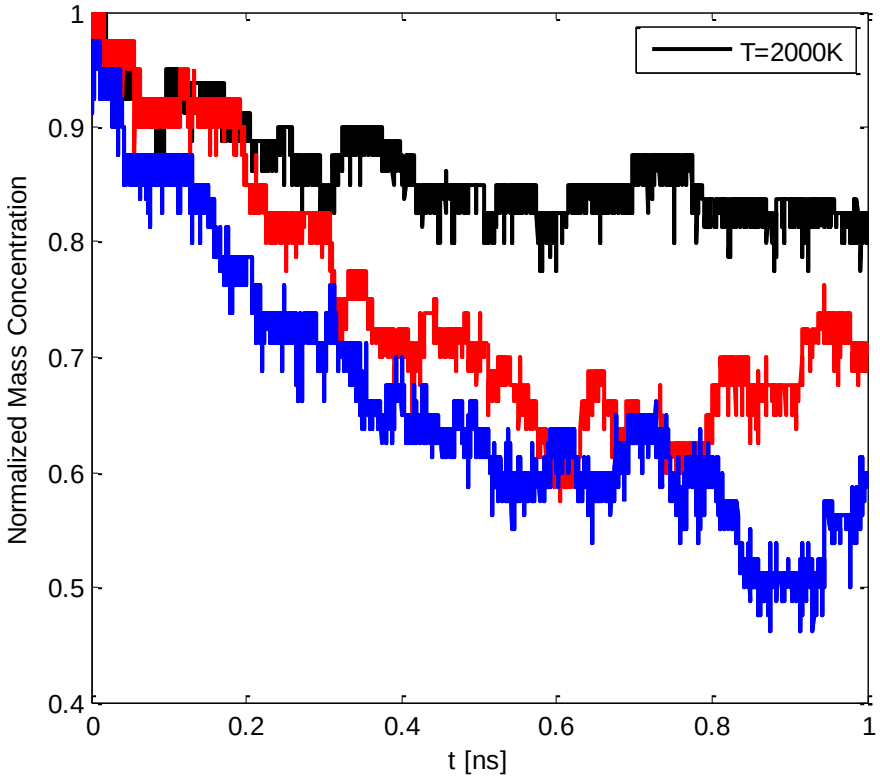

Figure 3: Normalized mass concentration of monomer versus simulation time for five values of temperature: 1000K (black), 1500K (red) , 2000K (green), 2300K (blue), 2500K (magenta). C_0=46g/L, pH=pK_{a1}.

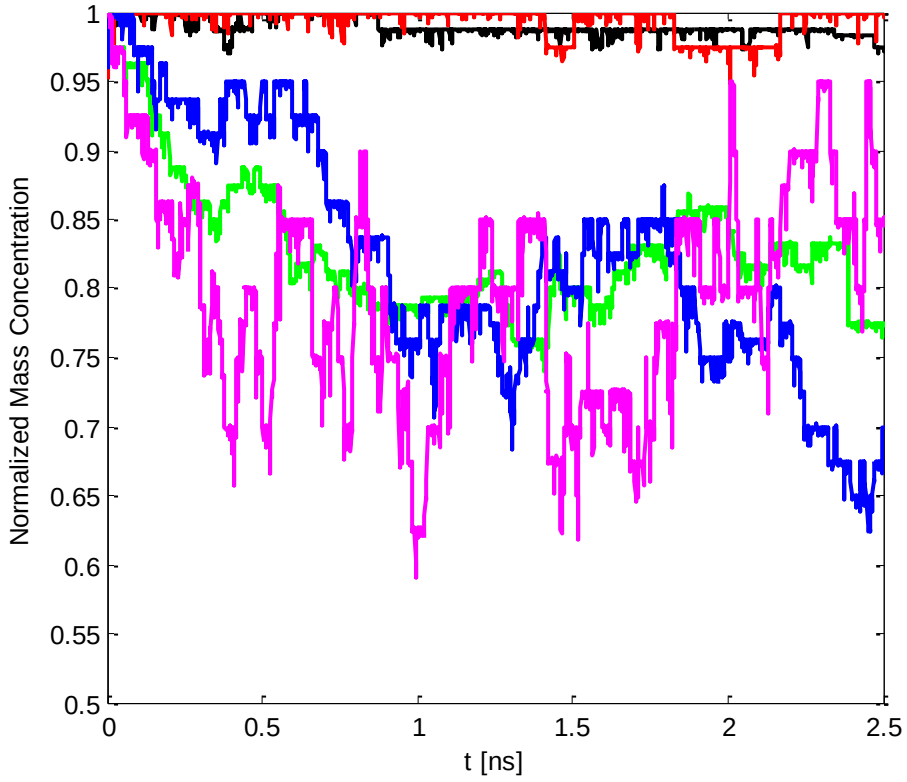

Figure 4: Normalized mass concentration of monomer versus simulation time for three values of temperature: 1000K (black), 1500K (red) , 2000K (green). C_0=115g/L, pH=pK_{a1}.

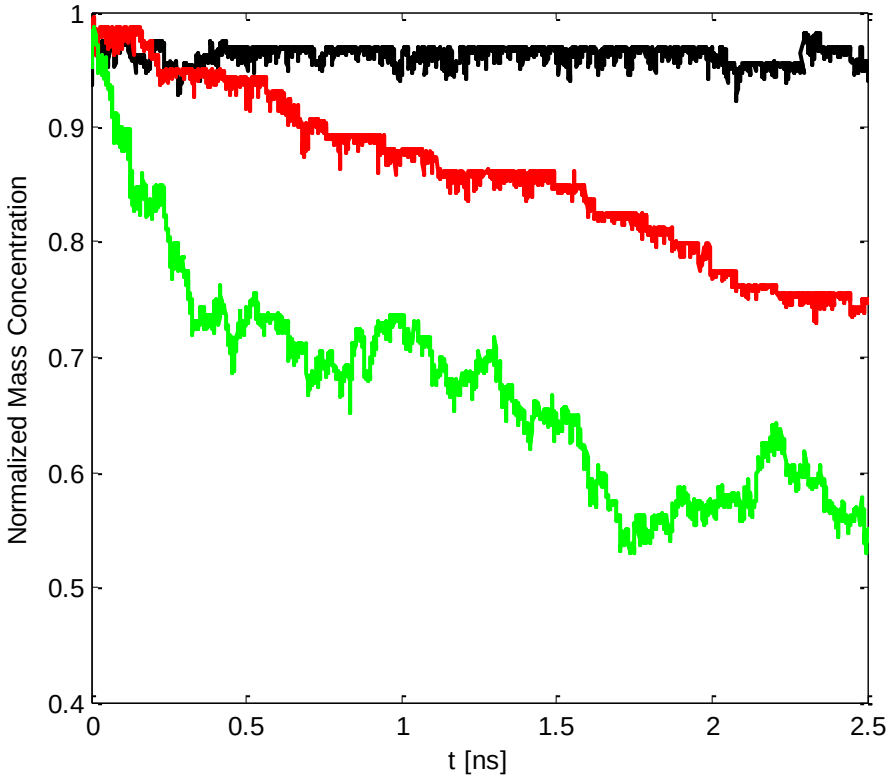

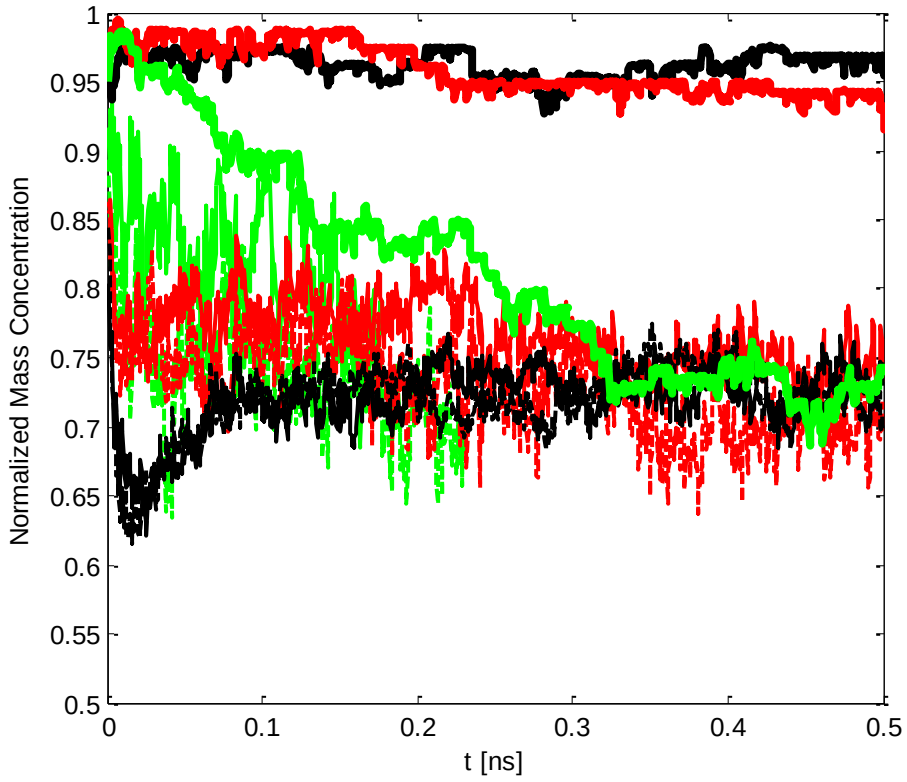

Figure 5: Normalized mass concentration of monomer versus simulation time for three values of water content and three values of temperature. C_0=115g/L, $R_{b/a}$=1.

T= 1000K (black), 1500K (red), 2000K (green)

n_{HS}=0 (dashed line, N_0=64), 1 (solid line, N_0=64), 29 (bold and solid line, N_0=160); Note that the system size doesn't change the results.

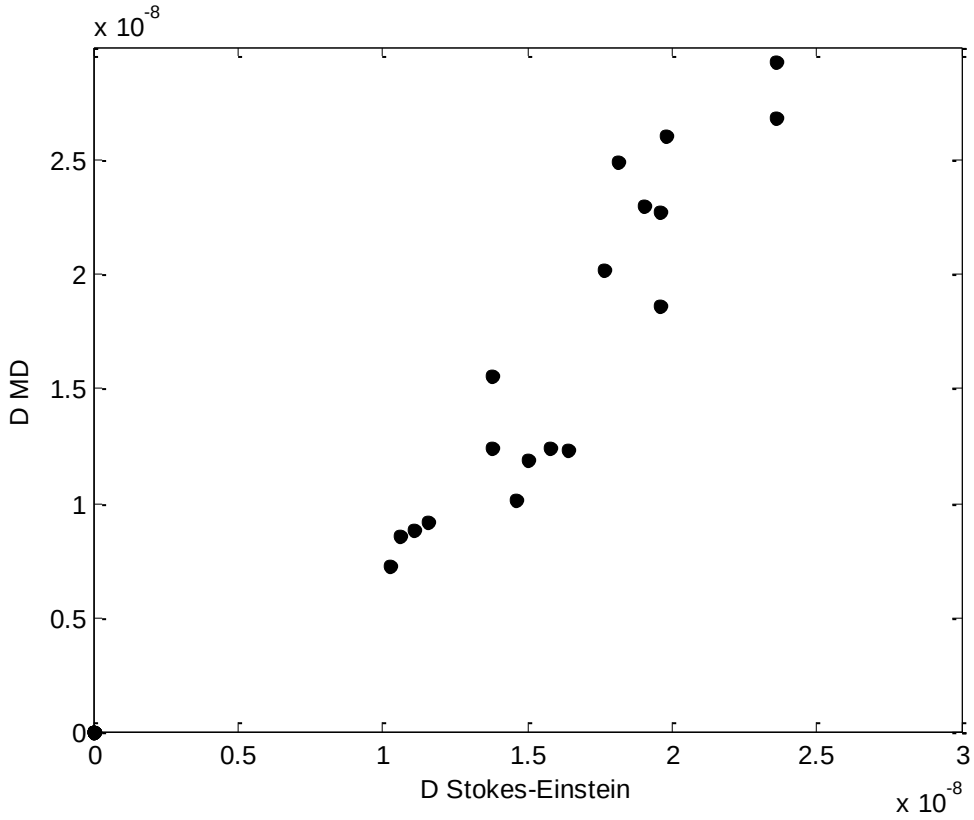

Figure 6: diffusion coefficient computed following Stokes-Einstein equation versus the one from MD simulations. Unit: m^2/s

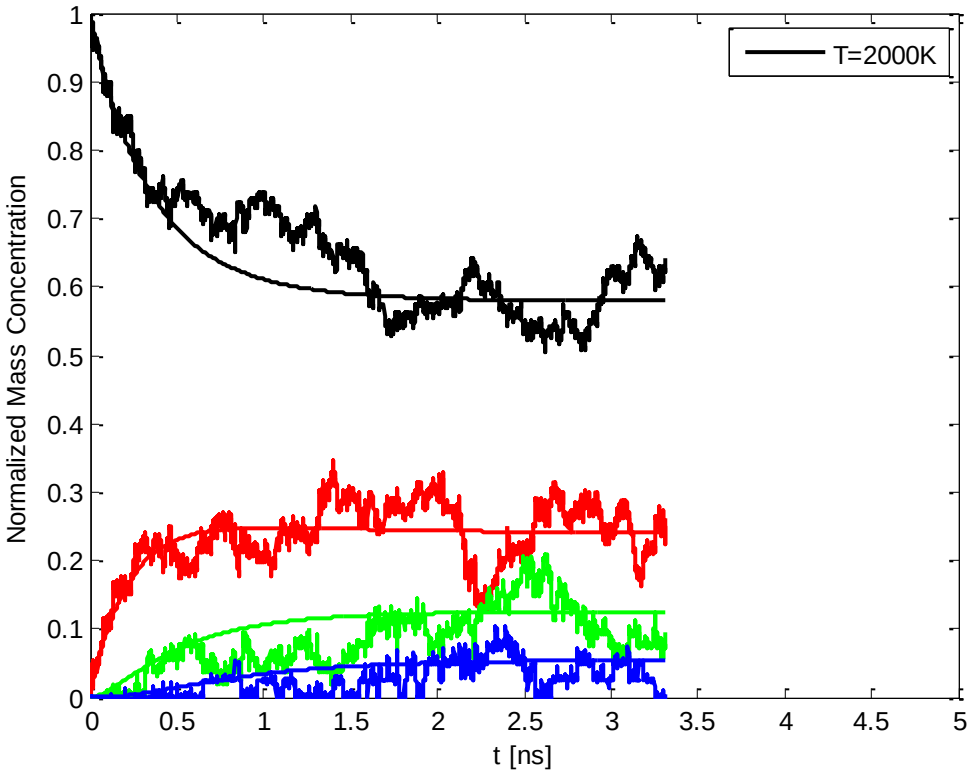

Figure 7a: normalized mass concentration of oligomer versus time (N_0=160, C_0=115g/L, $R_{b/a}$=1) for T=2000K.

black: monomer; red: dimer; green: trimer; blue: tetramer;

solid line: model; fluctuating line: MD-simulation

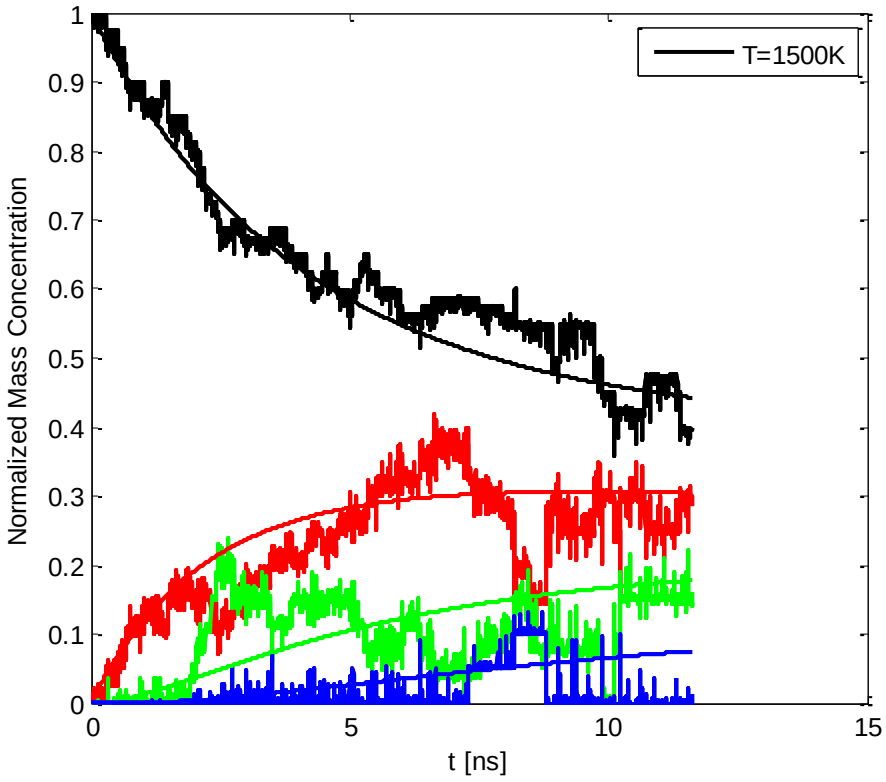

Figure 7b: normalized mass concentration of oligomer versus time (N_0=40, C_0=115g/L, $R_{b/a}$=1) for T=1500K.

black: monomer; red: dimer; green: trimer; blue: tetramer;

solid line: model; fluctuating line: MD-simulation

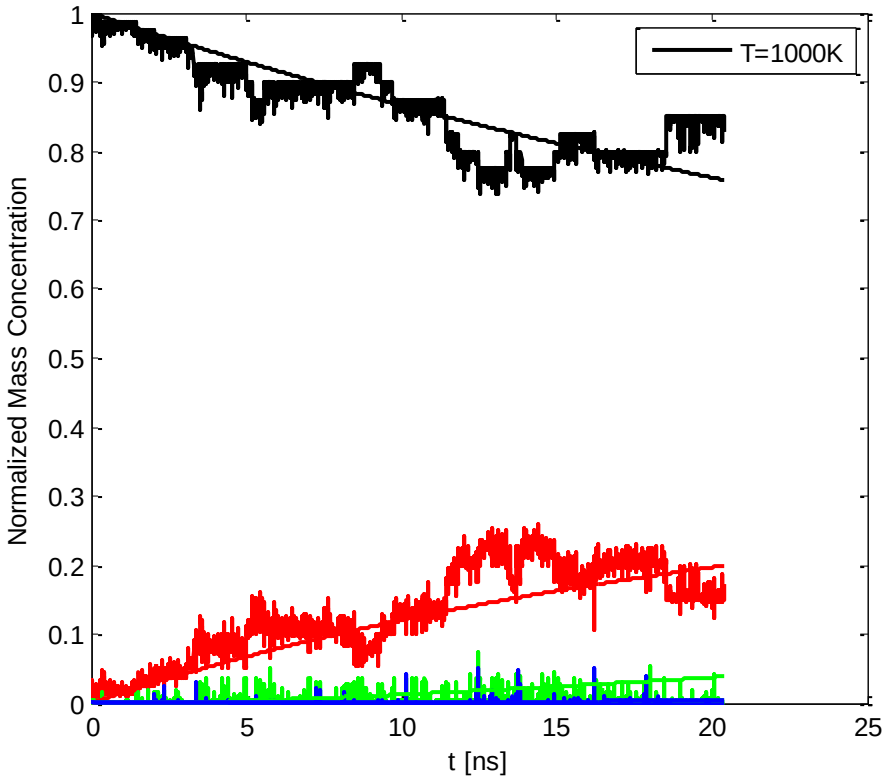

Figure 7c: normalized mass concentration of oligomer versus time (N_0=40, C_0=115g/L, $R_{b/a}$=1) for T=1000K.

black: monomer; red: dimer; green: trimer; blue: tetramer;

solid line: model; fluctuating line: MD-simulation

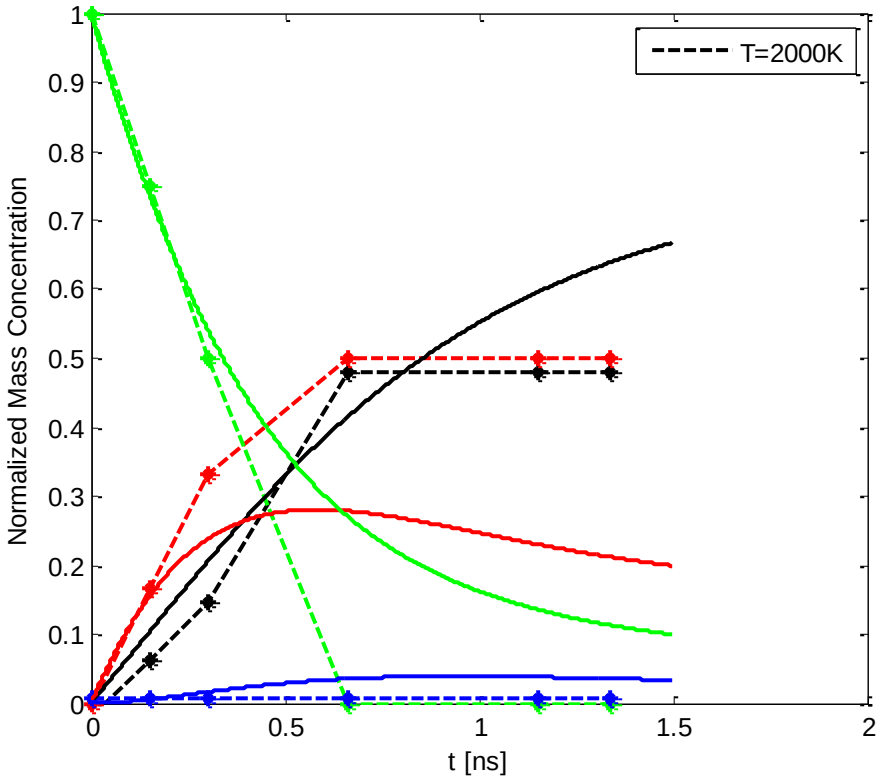

Figure 8: initial state: 4 trimer and 870 H_2O molecules

normalized mass concentration of oligomer versus time (C_0=46g/L; $R_{b/a}$=1) for T=2000K.

black: monomer; red: dimer; green: trimer; blue: tetramer;

solid line: model; dotted line: MD-simulation

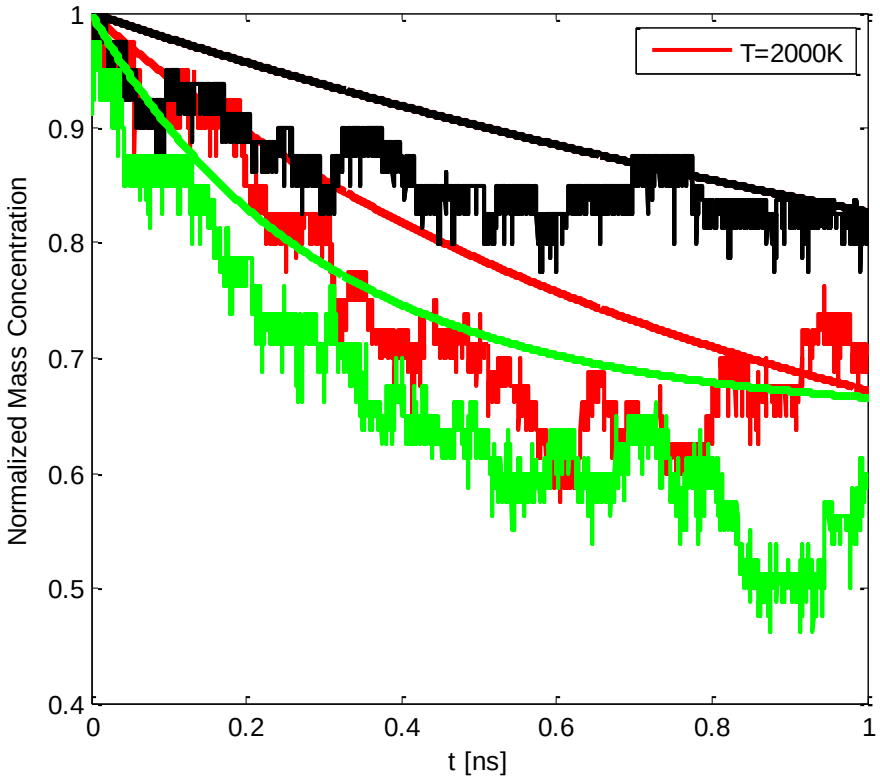

Figure 9: monomer concentration versus time for various values of $R_{b/a}$ or pH. T=2000K, C_0=115g/L.

MD simulation versus modelling (solid line)

(R, pH) values: (0.05, 8.2) (black), (0.16, 8.7) (red) and (1.58, 9.7) (green)

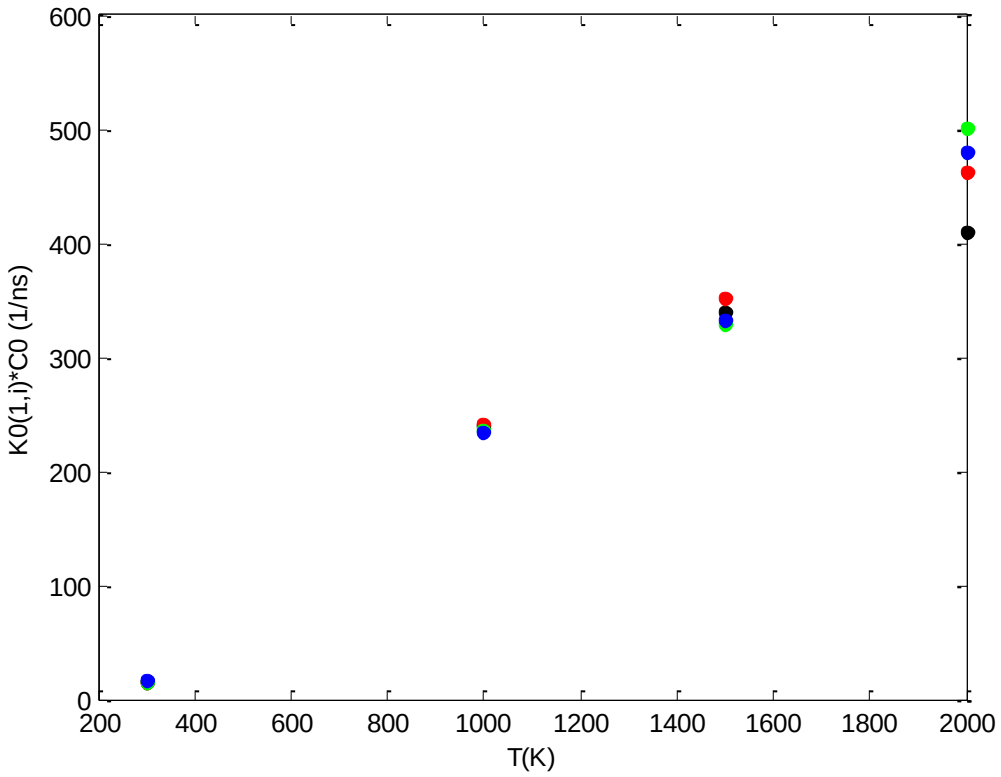

Figure 10: the pre-exponential term of the kinetic constant (normalized by $1/C_0$) of the monomer/oligomer reaction versus the temperature for several small oligomers:

i=1 (black dot) i=2 (red dot) i=5 (green dot) i=10 (blue dot)

Figure 11: normalized mass concentration versus time C_0=2M, T=298K, max(i)=10

Solid line: $pH_{initial}=pK_{a1}=9.5$, closed system

Dashed line: $pH_{initial}=pK_{a1}=9.5$, open system (pH = 9.5 along the process)

i=1: black i=2: red i=3: green i=4: blue

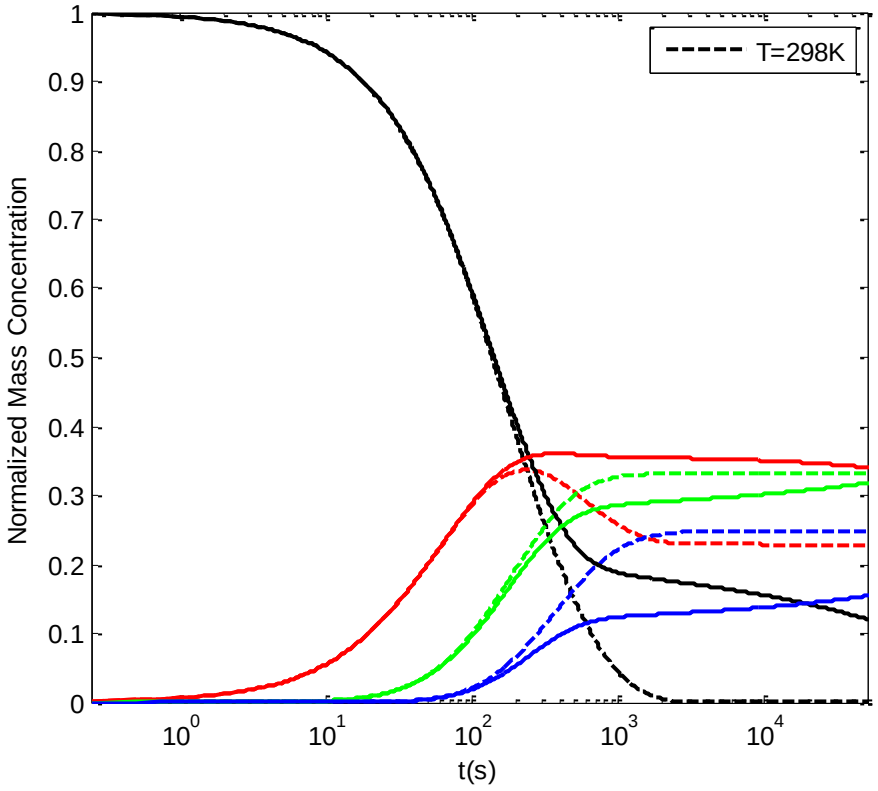

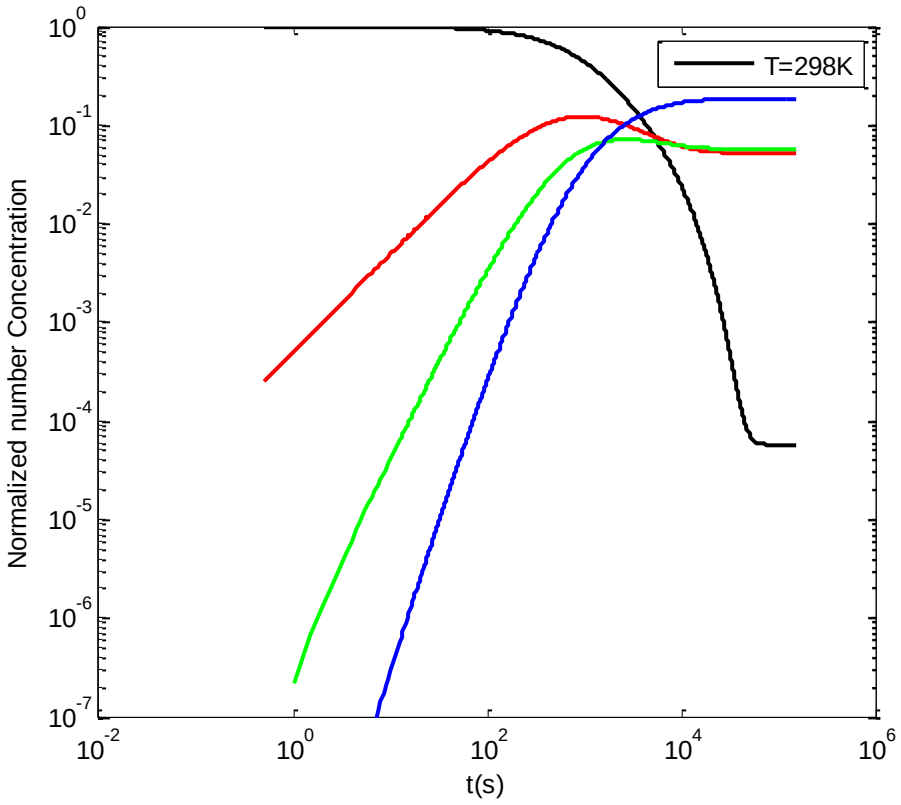

Figure 12: normalized number concentrations versus time

pH=8.5 C_0=1M T=298K, max(i)=4 ([50], figure 4)

i=1: black i=2: red i=3: green i=4: blue